

AD _____

Award Number:

W81XWH-07-1-0402

TITLE:

Role of PTEN in the Tumor Microenvironment

PRINCIPAL INVESTIGATOR:

Gustavo Leone, Ph.D

CONTRACTING ORGANIZATION:

The Ohio State University Research Foundation

Columbus, Oh 43210

REPORT DATE: June 2008

TYPE OF REPORT:

Annual

PREPARED FOR: U.S. Army Medical Research and Materiel Command
Fort Detrick, Maryland 21702-5012

DISTRIBUTION STATEMENT:

✓ Approved for public release; distribution unlimited

The views, opinions and/or findings contained in this report are those of the author(s) and should not be construed as an official Department of the Army position, policy or decision unless so designated by other documentation.

REPORT DOCUMENTATION PAGE				Form Approved OMB No. 0704-0188	
Public reporting burden for this collection of information is estimated to average 1 hour per response, including the time for reviewing instructions, searching existing data sources, gathering and maintaining the data needed, and completing and reviewing this collection of information. Send comments regarding this burden estimate or any other aspect of this collection of information, including suggestions for reducing this burden to Department of Defense, Washington Headquarters Services, Directorate for Information Operations and Reports (0704-0188), 1215 Jefferson Davis Highway, Suite 1204, Arlington, VA 22202-4302. Respondents should be aware that notwithstanding any other provision of law, no person shall be subject to any penalty for failing to comply with a collection of information if it does not display a currently valid OMB control number. PLEASE DO NOT RETURN YOUR FORM TO THE ABOVE ADDRESS.					
1. REPORT DATE (DD-MM-YYYY) 01-06-2008		2. REPORT TYPE Annual		3. DATES COVERED (From - To) 15 May 2007 - 14 May 2008	
4. TITLE AND SUBTITLE Role of PTEN in the Tumor Microenvironment				5a. CONTRACT NUMBER	
				5b. GRANT NUMBER W81XWH-07-1-0402	
				5c. PROGRAM ELEMENT NUMBER	
6. AUTHOR(S) Gustavo Leone, Ph.D.				5d. PROJECT NUMBER	
				5e. TASK NUMBER	
				5f. WORK UNIT NUMBER	
7. PERFORMING ORGANIZATION NAME(S) AND ADDRESS(ES) The Ohio State University Research Foundation Columbus, Oh 43210				8. PERFORMING ORGANIZATION REPORT NUMBER	
9. SPONSORING / MONITORING AGENCY NAME(S) AND ADDRESS(ES) U.S. Army Medical Research and Materiel Command Fort Detrick, Maryland 21702				10. SPONSOR/MONITOR'S ACRONYM(S)	
				11. SPONSOR/MONITOR'S REPORT NUMBER(S)	
12. DISTRIBUTION / AVAILABILITY STATEMENT Approved for public release					
13. SUPPLEMENTARY NOTES					
14. ABSTRACT Recent scientific advances have revealed that a malignant tumor can be viewed as an organ consisting of different types of interacting cells. Different tumor cell types play different roles in the growth and development of the tumor and thus in the end, all cells within the tumor may help pave the way for further tumor growth in a patient with cancer. Current work in the field indicates that fibroblasts surrounding breast cancers are particularly important for cancer progression, but no one knows why. Our experimental approach to this problem is a direct one; we target the mutation of genes in stromal fibroblasts surrounding the tumor in order to learn whether these genes are important for cancer progression. Using this approach we have shown that the Pten gene in fibroblasts is a major gene involved in suppressing epithelial breast cancers. In order to understand how <i>Pten</i> works in fibroblasts we will measure the immediate and long-term consequences of <i>Pten</i> mutation on the biology of all the cells surrounding the tumor, including the tumor cells themselves, as well as the matrix that holds these cells together. Because the entire system is so complex, we plan to study how the <i>Pten</i> gene behaves as a tumor suppressor by developing extremely detailed three-dimensional images of tumors where each image is annotated with detailed cancer related molecular information. This will allow us to use bioinformatics (computer assisted methods) to understand the molecular basis for how fibroblasts promote breast cancer. This information will lead to the design of novel therapeutic strategies that target fibroblasts and that could be used in combination with current therapies that target epithelial cells, to stop tumor growth and prevent reoccurrence or metastasis.					
15. SUBJECT TERMS Tumor microenvironment					
16. SECURITY CLASSIFICATION OF:			17. LIMITATION OF ABSTRACT UU	18. NUMBER OF PAGES 83	19a. NAME OF RESPONSIBLE PERSON USAMRMC
a. REPORT U	b. ABSTRACT U	c. THIS PAGE U			19b. TELEPHONE NUMBER (include area code)

Table of Contents

	<u>Page</u>
Introduction.....	4
Body.....	4
Key Research Accomplishments.....	6
Reportable Outcomes.....	7
Conclusion.....	7
References.....	8
Appendix-	9
Nature (Trimboli et al.) Article.....	13

INTRODUCTION:

Emerging evidence points to a particularly important role of **fibroblasts** within in the tumor stroma in promoting phenotypic changes that allow the extracellular matrix to evolve and contribute to the *invasiveness of epithelial tumor cells*. However, how stromal fibroblasts that promote cancer progression are poorly understood and are only beginning to emerge. The Leone laboratory has developed a system to conditionally manipulate the mouse genome in stromal fibroblasts of the mammary gland (*FSP-cre*). Using this genetic system we present preliminary data suggesting that *Pten* function in mammary stromal fibroblasts plays a critical role in the progression of *ErbB2*-initiated mammary epithelial tumors. The task at hand is to now genetically and biochemically identify the key '*stroma-specific*' tumor suppressor activities of *Pten*, and to then relate these stroma-specific functions to the structural and molecular events taking place during tumor progression.

The immense genetic and cellular diversity of the tumor microenvironment, however, has made the problem of cancer progression difficult to address by traditional experimental approaches. The Leone and Saltz groups have therefore joined expertise to develop novel *genetic* and *high-resolution 3D bioinformatics models* that integrate *spatial* and *molecular* information relating to the genetics and biochemical properties of the tumor microenvironment. These models will provide an effective platform for identifying the relationships between the different cell compartments of the tumor microenvironment that are critical for cancer progression. The proposed studies will fall into two major efforts, each divided into two phases. The first major effort involves the genetic analysis of *Pten* in mouse tumor models. The progress report outlined below describes the progress made in this phase of the study. The work is now being prepared for publication.

BODY:

Coordinated signaling between different cell types of the '*normal stroma*' is required during embryonic and adult development (Wiseman BS, Werb Z, 2002.). While cellular and ECM activities of the stroma are maintained in balance throughout development, they can be appropriately activated in response to extreme but normal physiological cues, such as wounding, inflammation or pregnancy (Schedin P. 2006). The stroma can also be inappropriately activated, such as in cancer (Nelson CM, Bissell MJ. 2006). Fibroblasts are a principal constituent of the stroma responsible for the synthesis of growth and survival factors, chemokines, structural components of the ECM and enzymes that control its turnover. In breast tumors, stromal fibroblasts are believed to adapt and continuously co-evolve along with tumor epithelial cells (Littlepage et al., 2005). Fibroblasts are implicated in fostering transformation and tumor growth by providing factors that induce epithelial cell proliferation, ECM remodeling and blood vessel recruitment (Bhowmick et al., 2004b; Mueller and Fusenig, 2004; Kalluri and Zeisberg, 2006). Despite extensive evidence for a role of the tumor stroma in carcinogenesis, relatively little is known about the signaling pathways involved in the communication between the different cellular compartments of the tumor microenvironment that contribute to the cancer phenotype.

Phosphatase and tensin homolog (*PTEN*) is a tumor suppressor with lipid and protein phosphatase activity (Myers et al., 1998) that impacts several signaling pathways, including phosphoinositide 3-kinase (PI3K), and Ras-MAPK-Erk1/2 signaling pathways. *Pten* inactivation in mice and humans leads to a disruption in cell polarity, cell architecture, and chromosomal integrity as well as in the promotion of cell cycle progression, cell growth and stem cell self-renewal (Di Cristofano and Pandolfi, 2000). Not surprisingly, it's somatic or germ-line inactivation contributes to the genesis of many tumor types primarily epithelial in origin. While tremendous progress in understanding PTEN function in tumor cells has been made since its discovery over a decade ago, relatively little is known about its potential role in the tumor stroma. Patients with Cowden syndrome have germline mutations in *PTEN*, suggesting that the higher risk for developing breast cancer in these patients could be due to *PTEN* activity in either epithelial or stromal compartments. Here, we have generated a mesenchymal-specific *Fsp-cre* transgene and conditional alleles of *Pten* (*Pten^{loxP}*) in mice to ablate its function in mammary stromal fibroblasts *in vivo* and rigorously evaluate its role in the tumor microenvironment. We show that *Pten* ablation in mammary stromal fibroblasts results in the induction and activation of Ets2-P(T72), massive remodeling of the ECM, recruitment of innate immune cells, and enhanced progression and malignancy of mammary tumors of epithelial origin. These findings expand *Pten*'s repertoire as a tumor suppressor by identifying the fibroblast as a key site from which it exerts its powerful tumor suppressive influence on adjacent epithelium.

For well over a century, the pathology of cancer suggested that malignant tumors consist of a complex cellular system dependent on reciprocal signaling between tumor cells and the adjacent stroma. The signaling pathways involved in the communication between the various cell types in the tumor remain virtually unknown. We recently developed a mesenchymal-specific *cre* mouse and used it here to target the inactivation of *Pten* in mammary stromal fibroblasts of the mammary gland and examine, for the first time, its role in the tumor microenvironment *in vivo*. This work identified the Pten-Ets2 pathway as a key regulatory axis in stromal fibroblasts that profoundly attenuates malignant characteristics of the tumor microenvironment and suppresses mammary epithelial tumors.

The tumor suppressor functions of Pten have been extensively studied in the tumor cell, but whether it also plays a role in other cell compartments of the tumor was unknown. We show direct *in vivo* evidence for a critical tumor suppressor role of *Pten* in the tumor microenvironment. Genetic ablation of *Pten* in stromal fibroblasts of the mammary gland resulted in a dramatic perturbation of the tumor microenvironment by increasing ECM deposition and a host of activities imbedded in it that together favor the initiation and progression of mammary epithelial tumors. This novel function of Pten in maintaining homeostasis within the mammary microenvironment may also be relevant in the suppression of epithelial tumors of other organs. Such a role for Pten may extend beyond cancer, to conditions where the microenvironment is speculated to profoundly impact disease manifestation including in autoimmune syndromes, lung fibrosis and neurodegeneration. Interestingly, the stromal *Pten* expression signature identified here includes genes that have been causally linked with ECM deposition and inflammation in rheumatoid arthritis, lung fibrosis and neurodegeneration.

KEY RESEARCH ACCOMPLISHMENTS:

TASK 1 (month 3- 18): Paper in re-submission to *Nature* (Trimboli et al.) attached.

TASK 2 (months 3-18): Work dealing with *Pten* in progress. Paper in progress (Hui Wang et al.). Work behind approximately 8 months.

TASK 3 (month 12-18): See *Nature* (Trimboli et al.) article attached. This task is addressed in this article.

TASK 4 (month 18-24):Partly completed. Also addressed in *Nature* (Trimboli et al.) article attached. The component dealing with regional areas of stroma (macrophages) is ongoing.

TASKS 5-7 (month 1- 24): Work on these tasks is ongoing. The no cost extension is requested to complete this important component of this project. The “segmentation” component (see figure 1 below) has encountered significant technical hurdles dealing with image segmentation, but even so, we feel that these can be overcome in the next 6 months.

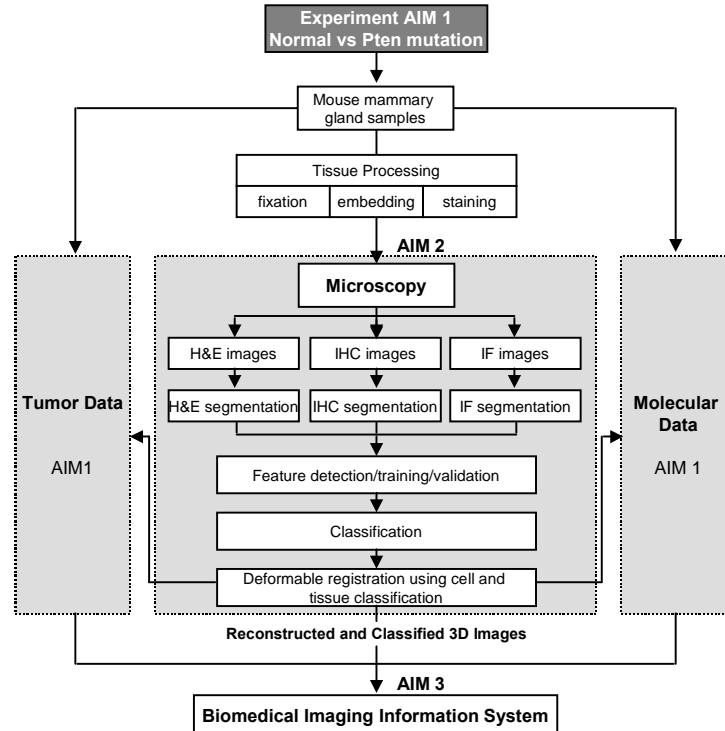


Figure 1: Scientific Processes Involved in Creation of BIIS

REPORTABLE OUTCOMES:

1. Manuscripts in preparation
 - A. Trimboli et al. *Pten* in Stromal Fibroblasts Suppresses Mammary Epithelial Tumors.
 - B. Cantemir et al. Tumor Fibroblasts and Ets2 Regulate Angiogenesis in Breast Cancer.
2. Submitted an NCI grant application (U01) that is related to this work.

CONCLUSIONS:

The mechanism by which Pten in the stroma regulates the expression of such an extensive set of genes likely involves complex transcriptional networks. The importance of the Pten-Ets2 axis in stromal fibroblasts is consistent with previous work from Oshima and colleagues that showed a critical cell non-autonomous role for Ets2 in mammary tumor growth (Tynan et al. 2005). Moreover, analysis of tumor-stroma gene expression signatures identified Ets2 activation as a key event associated with breast cancer patients having the worst prognosis (Park et al., 2007). In summary, this study offers a molecular basis for how altered signaling from the tumor stroma contributes to the most malignant characteristics of the breast cancer phenotype.

REFERENCES

1. [Wiseman BS, Werb Z.](#) (2002). Stromal effects on mammary gland development and breast cancer. *Science* 296, 1046-1049
2. [Schedin P.](#) (2006) Pregnancy-associated breast cancer and metastasis. *Nat Rev Cancer.* 6, 281-291.
3. [Nelson CM, Bissell MJ.](#) (2006). Of extracellular matrix, scaffolds, and signaling: tissue architecture regulates development, homeostasis, and cancer. *Annu Rev Cell Dev Biol.*, 287-309.
4. [Littlepage LE, Egeblad M, Werb Z.](#) (2005). Coevolution of cancer and stromal cellular responses. *Cancer Cell* 7, 499-500.
5. [Bhowmick NA, Neilson EG, Moses HL.](#) (2004b). Stromal fibroblasts in cancer initiation and progression. *Nature* 432, 332-337.
6. [Mueller MM, Fusenig NE.](#) (2004). Friends or foes - bipolar effects of the tumour stroma in cancer. *Nat Rev Cancer* 4, 839-849.
7. [Kalluri R, Zeisberg M.](#) (2006). Fibroblasts in cancer. *Nat Rev Cancer.* 6, 392-401.
8. [Myers MP, Pass I, Batty IH, Van der Kaay J, Stolarov JP, Hemmings BA, Wigler MH, Downes CP, Tonks NK.](#) (1998). The lipid phosphatase activity of PTEN is critical for its tumor suppressor function. *Proc Natl Acad Sci U S A* 95, 13513-13518.
9. Di Cristofano A, Pandolfi PP. (2000). The multiple roles of PTEN in tumor suppression. *Cell* 100, 387-390.
10. [Tynan JA, Wen F, Muller WJ, Oshima RG.](#) (2005). Ets2-dependent microenvironmental support of mouse mammary tumors. *Oncogene* 24, 6870-6876.
11. [Park ES, Lee JS, Woo HG, Zhan F, Shih JH, Shaughnessy JD Jr, Frederic Mushinski J.](#) (2007). Heterologous tissue culture expression signature predicts human breast cancer prognosis. *PLoS ONE* 2, e145.

1. **Leone, G.**, Maybaum, L. And Lee, P.W.K. (1992). The Reovirus cell attachment protein possesses two independently active trimerization domains: Basis of dominant negative effects. ***Cell*** 71:479-488.
2. DeGregori, J.*, **Leone, G.***, Ohtani, K., Miron, A. and Nevins, J.R. (1995) E2F1 accumulation bypasses a G₁ arrest resulting from the inhibition of G₁ cyclin-dependent kinase activity. ***Genes & Development***, 9:2873-2887. *These authors contributed equally to this work.
3. Gilmore, R., Coffey, M., **Leone, G.**, McLure, K., Lee, P.W.K. (1996). Co-translational trimerization of the Reovirus cell attachment protein. ***The EMBO Journal*** 15(11):2651-2658.
4. **Leone, G.**, Coffey, M., Gilmore, R., Duncan, R., and Lee, P.W.K. (1996) C-terminal Trimerization, but not N-terminal trimerization, of the Reovirus cell attachment protein is a post-translational and hsp70/ATP dependent process. ***J. Biol. Chem.*** 271 (14):8466-8471.
5. DeGregori, J., **Leone, G.**, Miron, A., Jakoi, L., and Nevins, J.R. (1997). Distinct roles for E2F proteins in cell growth control and apoptosis. ***Proc. Natl. Acad. Sci. USA.*** 94, 7245-7250.
6. **Leone, G.**, DeGregori, J., Sears, R., Jakoi, L., and Nevins, J.R. (1997). Myc and Ras collaborate in inducing accumulation of active cyclin E/Cdk2 and E2F. ***Nature.*** 387, 422-425.
7. **Leone, G.**, DeGregori, J., Yan, Z., Jakoi, L., Ishida, S., Williams, R.S., Nevins, J.R. (1998). E2F3 activity is regulated during the cell cycle and is required for the induction of S phase. ***Genes & Development.*** 12:2120-2130.
8. Sears, R., **Leone, G.**, DeGregori, J., and Nevins, J.R. (1999). Ras enhances Myc protein stability. ***Molecular Cell.*** 3:169-179.
9. **Leone, G.**, DeGregori, J., Jakoi, L., Cook, J.G., and Nevins, J.R. (1999). Collaborative role of E2F transcriptional activity and G1 cyclin-dependent kinase activity in the induction of S phase. ***Proc. Natl. Acad. Sci. USA.*** 96:6626-6631.
10. **Leone, G.**, Nuckolls, F., Ishida, S., Adams, M., Sears, R., Jakoi, L., Miron, A., Nevins, J.R. (2000) Identification of a novel E2F3 product suggests a mechanism for determining specificity of repression by Rb proteins. ***Mol. Cell. Biol.*** 20:10, 3626-3632
11. **Leone G.**, Sears R., Huang E., Rempel R., Nuckolls F., Park C., Giangrande P., Wu L., Saavedra H.I., Field S.J., Thompson M.A., Yang H., Fujiwara Y., Greenberg M.E., Orkin S., Snith C., and Nevins J.R. (2001). Myc requires distinct E2F activities to induce S phase and apoptosis. ***Molecular Cell,*** 8: 105-113.
12. Wu L., Timmers C., Baidehi M., Saavedra H.I., Sang L., Chong G.T., Nuckolls F., Giangrande P., Wright F.A., Field S.J., Greenberg M.E., Orkin S., Nevins J.R., Robinson M.L., and **Leone G.** (2001). The E2F1-3 transcription factors are essential for cellular proliferation. ***Nature,*** 414:457-462.
13. Cook J.G., Park C., Burke T.W., **Leone G.**, DeGregori J., Engel A., and Nevins J.R. (2002). Analysis of Cdc6 function in the assembly of mammalian prereplication complexes. ***Proc. Natl. Acad. Sci., USA,*** 99:3 1347-1352.
14. Saavedra H.I., Wu L., de Bruin A., Timmers C., Rosol T.R., Weinstein M., Robinson M.L., and **Leone G.** (2002). Specificity of E2F1, E2F2 and E2F3 in mediating phenotypes induced by loss of Rb. ***Cell Growth & Differentiation*** (13:5 215-225). Cover of Journal.
15. Wu L., de Bruin A., Saavedra H.I., Trimboli A., Yang Y., Opavska J., Wilson P., Starovic M., Ostrowski M.C., Cross J.C., Weinstein M., Rosol T.J., Robinson M.L., and **Leone G.** (2003). Extraembryonic function of Rb is essential for embryonic development and viability. ***Nature*** 421: 942-947. (N&V; 421: 903-004)
16. Saavedra H.I., Maiti B., Timmers C., Altura R., Fukasawa K., and **Leone G.** (2003). Inactivation of E2F3 results in premature centriole separation and centrosome amplification. ***Cancer Cell*** 3: 333-346 (Cover).

17. de Bruin A., Wu L., Saavedra H.I., Wilson P., Yang Y., Weinstein M., Rosol T.J., Robinsom M.L., **Leone G.** (2003). Rb function in extraembryonic lineages is critical for the control of apoptosis in the central nervous system of Rb-deficient mice. **Proc. Natl. Acad. Sci. USA**, 100:11 6546-6551.
18. de Bruin A, Maiti B, Jakoi L, Timmers C, and **Leone G.** (2003). Identification and Characterization of E2F7, a Novel Mammalian E2F Family Member Capable of Blocking Cellular Proliferation. **J. Biol. Chem.** 278:43, 42041-42049.
19. Zhang J, Gray J, Wu L, **Leone G.**, Rowan S, Cepko CL, Zhu X, Craft CM, Dyer MA. (2004). Rb regulates proliferation and rod photoreceptor development in the mouse retina. **Nature Genetics** 36:4 1-10.
20. Jiang Y., Saavedra H.I., Holloway M.P., **Leone G.**, Altura RA. (2004). Aberrant Regulation of Survivin by the Rb/E2F Family of Proteins. **J. Biol. Chem** 279, 40511-40520.
21. Iavarone A., King E.R., Dai X., **Leone G.**, Stanley E.R., Lasorella A. (2004). Retinoblastoma promotes definitive erythropoiesis by repressing Id2 in fetal liver macrophages. **Nature** 432: 1040-1045.
22. Maiti B., Li J., de Bruin A., Gordon F., Timmers C, Opavsky R., Patil K., Tuttle J., Cleghorn W., and **Leone G.** (2005). Cloning and Characterization of Mouse E2F8, a Novel Mammalian E2F Family Member Capable of Blocking Cellular Proliferation. **J. Biol. Chem.** 280, 18211-18220.
23. Logan N., Graham A., Zhao X., Fisher R., Maiti B., **Leone G.**, La Thangue N. (2005). E2F-8: an E2F family member with a similar organization of DNA binding domains to E2F-7. **Oncogene** 24,5000-5004.
24. Sharma N., Timmers C., Trikkha P., Saavedra, H., Obery, A., and **Leone, G.** (2006). Control of the p53-p21^{CIP1} axis by *E2f1*, *E2f2* and *E2f3* is essential for G₁/S progression and cellular transformation. **J. Biol. Chem** 281:36124-31.
25. Dorrance, A, Liu, S., Yuan, W., Becknell, B., Arnoczky, K., Guimond, M., Strout, M., Feng, L., Nakamura, T., Yu, L., Rush, L., Weinstein, M., **Leone, G.**, Wu, L., Ferketich, A., Whitman, S., Marcucci, G., and Caligiuri, M., (2006). The *Mll* partial tandem duplication includes aberrant *Hox* expression in vivo via specific epigenetic alterations. **J. Clin. Invest.** 116:65-78.
26. Timmers C., Opavsky R., Maiti B., Wu L., Wu J., Orringer D., Sharma N., Saavedra H.I., **Leone G.** (2007). E2F1-3 controls a p53-dependent checkpoint that is essential for cellular proliferation. **Mol Cell Biol.** 1:65-78.
27. Wenzel, P., Wu, L., de Bruin, A., Chong, J-L, Chen, W-Y., Dureska, G., Sites, E., Pan, T., Sharma, A., Huang, K., Ridgway R., Mosaliganti K., Sharp, R., Machiraju, R., Saltz, J., Yamamoto, H., Cross, J., Robinson, M., and **Leone, G.** (2007). Rb is critical in a mammalian tissue stem cell population. **Genes & Development** 21:85-97.
28. Wenzel, P., **Leone, G.** (2007). Expression of Cre recombinase in early diploid trophoblast cells of the mouse placenta. **Genesis**. 45:129-34.
29. McClellan K., Ruzhynsky V., Douda D., Vanderluit J., Ferguson K., Chen D., Bremner R., Park D., **Leone G.**, and Slack R. (2007). Unique requirement for Rb/E2F3 in neuronal migration: evidence for cell cycle-independent functions. **Mol Cell Biol** 27:4825-43.
30. Chen D., Opavsky R., Pacal M., Tanimoto N., Wenzel P., Seeliger M., **Leone G.**, and Bremner R. (2007). Rb-mediated neuronal differentiation through cell cycle independent regulation of E2f3a. **PLoS Biology** 5:e179 1-16.
31. Opavsky R., Wang S-H., Trikha P., Raval A., Huang Y., Wu Y-A., Rodriguez B., Keller B., Liyanarachi S., Wei G., Davuluri R., Weinstein M., Felsher D., Ostrowski M.C., **Leone G***, and Plass C*. (2007). CpG island methylation in cancer is driven by the genetic configuration of tumor cells. **PLoS Genetics** 3:1757-69. *corresponding authors
32. Opavsky R., Tsai S-Y., Guimond M., Arora A., Opavska J., Becknell B., Kauffman M., Walton N., Stephens J., Fernandez S., Muthusamy N., Felsher W., Porcu P., Caligiuri M., and **Leone G.** (2007). Specific tumor suppressor function for E2F2 in Myc-induced T cell lymphomagenesis. **Proc. Natl. Acad. Sci. USA** 104:39, 15400-15405.

***Pten* in Stromal Fibroblasts Suppresses Mammary Epithelial Tumors**

Anthony J. Trimboli^{1,2*}, Carmen Z. Cantemir-Stone^{3*}, Fu Li^{1,3*}, Julie A. Wallace³, John C. Thompson^{1,2}, Enrico Caserta^{1,2}, Anand Merchant³, Nicholas Creasap^{1,2}, Jean-Leon Chong^{1,2}, Shan Naidu^{1,2,4}, Guo Wei^{1,3}, Sudarshana M. Sharma³, Parul Gulati⁵, Julie A. Stephens⁵, Soledad A. Fernandez⁵, Metin N. Gurcan⁶, Michael B. Weinstein^{1,2}, Francois Pepin^{7,8}, Michael Hallett^{7,8}, Morag Park^{7,9}, Thomas J. Rosol⁴, Paul C. Stromberg⁴, Michael L. Robinson^{10#}, Michael C. Ostrowski^{3,¶} and Gustavo Leone^{1,2,¶}

¹Department of Molecular Genetics, College of Biological Sciences; ²Department of Molecular Virology, Immunology and Medical Genetics, ³Department of Molecular and Cellular Biochemistry, College of Medicine; ⁴Department of Veterinary Biosciences, College of Veterinary Medicine; ⁵Center for Biostatistics, Office of Health Sciences; ⁶Department of Biomedical Informatics, School of Medicine, The Ohio State University, Columbus, OH 43210; ⁷Department of Biochemistry, Rosalind and Morris Goodman Cancer Center, ⁸McGill Center for Bioinformatics, ¹¹Department of Oncology, McGill University, Québec H3A 1A1, Canada; ⁹Center for Molecular and Human Genetics, Columbus Children's Research Institute, Columbus, OH 43205; ¹³Tumor Microenvironment Program, Comprehensive Cancer Center, The Ohio State University, Columbus, OH 43210.

Running title: Pten-Ets2 tumor suppressor axis in stromal fibroblasts

* These authors contributed equally to this study

Current address: Department of Zoology, Miami University, Oxford, OH 45056

¶ Corresponding Author Information:

Gustavo Leone
Department of Molecular Genetics
Department of Molecular Virology,
Immunology and Medical Genetics
Tumor Microenvironment Program
The Ohio State University
808 Biomedical Research Tower
460 W. 12th Ave.
Columbus, OH 43210
Telephone: 614-688-4567
FAX: 614-688-4181
e-mail: gustavo.leone@osumc.edu

Michael C. Ostrowski
Department of Molecular & Cellular
Biochemistry
Tumor Microenvironment Program
The Ohio State University
810 Biomedical Research Tower
460 W. 12th Ave.
Columbus, OH 43210
Telephone: 614-688-3824
FAX: 614-688-4181
e-mail: michael.ostrowski@osumc.edu

SUMMARY

The tumor stroma is believed to contribute to some of the most malignant characteristics of epithelial tumors. However, signaling between stromal and tumor cells is complex and remains poorly understood. Here we show that the genetic inactivation of *Pten* in stromal fibroblasts of mouse mammary glands accelerated the initiation, progression and malignant transformation of mammary epithelial tumors. This was associated with the massive remodeling of the extra-cellular matrix (ECM), innate immune cell infiltration and increased angiogenesis. Loss of *Pten* in stromal fibroblasts led to increased expression, phosphorylation (T⁷²) and recruitment of Ets2 to target promoters known to be involved in these processes. Remarkably, *Ets2* inactivation in *Pten* stroma-deleted tumors ameliorated disruption of the tumor microenvironment and was sufficient to decrease tumor growth and progression. Global gene expression profiling of mammary stromal cells identified a Pten-specific signature that was highly represented in the tumor stroma of breast cancer patients. These findings identify the Pten-Ets2 axis as a critical stroma-specific signaling pathway that suppresses mammary epithelial tumors.

Coordinated signaling between different cell types of the ‘*normal stroma*’ is required during embryonic and adult development¹. The stroma can be appropriately activated in response to extreme but normal physiological cues, such as wound, inflammation or pregnancy². The stroma can also be inappropriately activated in cancer^{3, 4}. In breast tumors, stromal fibroblasts are believed to adapt and continuously co-evolve along with tumor epithelial cells in order to foster transformation and tumor growth⁵. Fibroblasts are a principal constituent of the stroma responsible for the synthesis of growth and survival factors, angiogenic and immunological chemokines, and structural components of the ECM as well as enzymes that control its turnover^{6, 7}. Despite extensive evidence for a role of the tumor stroma in carcinogenesis, relatively little is known about the signaling pathways involved in the communication between the different cellular compartments of the microenvironment that contribute to the cancer phenotype.

Alterations in the phosphoinositide 3-kinase (PI3K) pathway are associated with the activation of tumor-associated stroma^{8, 9}. One of the main regulators of PI3K signaling is the phosphatase and tensin homolog (*PTEN*), a tumor suppressor with lipid and protein phosphatase activity^{10, 11}. *PTEN* inactivation disrupts multiple cellular processes associated with cell polarity, cell architecture, chromosomal integrity, cell cycle progression, cell growth and stem cell self-renewal^{12, 13}. Germ-line inactivation of a single allele of *PTEN* in both human and mice contributes to the genesis of a variety of tumor types of epithelial origin¹⁴. While tremendous progress in understanding *PTEN* function in tumor cells has been made since its discovery over a decade ago, relatively little is known about its potential role in the tumor stroma. Here, we show that *Pten* ablation in mammary stromal fibroblasts of mice results in massive remodeling of the

ECM and tumor vasculature, recruitment of innate immune cells, and increased malignancy of mammary epithelial tumors. Gene expression profiling of *Pten*-deleted stromal fibroblasts identified an *Ets2*-specific transcription program associated with many of these aggressive tumor phenotypes. Remarkably, the concomitant inactivation of *Ets2* in the mammary stroma reversed the increased malignancy caused by *Pten* deficiency. These findings expand *Pten*'s repertoire as a tumor suppressor by identifying the fibroblast as a key site from which it exerts its powerful tumor suppressive influence on the adjacent tumor epithelium.

RESULTS

***Pten* in stromal fibroblasts suppresses mammary tumors of epithelial origin**

To rigorously evaluate the role of *Pten* in the tumor microenvironment of breast cancer we generated mice containing a mesenchymal-specific *Fsp-cre* transgene¹⁵ and conditional alleles of *Pten* (*Pten*^{loxP}; Supplementary Fig. 1). Cell type-marker analysis using a β -galactosidase *Rosa26*^{LoxP} reporter allele showed specific *Fsp-cre* expression in stromal fibroblasts surrounding the mammary epithelial ducts, with no expression in cytokerin-positive epithelial cells, F4/80-positive macrophages and CD31-positive endothelial cells (Fig. 1a, Supplementary Fig. 2a, 2b). Southern, PCR and Western blot assays demonstrated efficient cre-mediated deletion of *Pten*^{loxP} in stromal fibroblasts isolated from *Fsp-cre;Pten*^{loxP/loxP} mammary glands (data not shown and Fig. 1b, 1c). Examination of mammary sections by immunohistochemistry (IHC) showed deletion of *Pten*^{loxP} that was confined to stromal fibroblasts, with no collateral deletion in epithelial ducts or the adjacent myoepithelium (Fig. 1d, Supplementary Fig. 3a, 3b). Interestingly,

this resulted in the expansion of the ECM, but did not lead to the transformation of the mammary epithelium (Fig 1d, 2b).

We then examined the role of stromal *Pten* on mammary tumorigenesis using two established mouse models of breast cancer, *MMTV-ErbB2/neu* (*ErbB2*)¹⁶ and *MMTV-rtTA;teto-MYC* (*MYC*)^{17, 18}. While not representative of all known genetic abnormalities in breast cancer, these two mouse models have unique molecular, cellular and clinical features that can be used to evaluate different aspects of this heterogeneous disease. To avoid possible confounding effects caused by *Pten* deletion in mesenchymal cells of other organs, mammary glands from *Fsp-cre;Pten^{loxP/loxP}* (n=5), *ErbB2;Pten^{loxP/loxP}* (n=12), *MYC;Pten^{loxP/loxP}* (n=20), *ErbB2;Fsp-cre;Pten^{loxP/loxP}* (n=16) and *MYC;Fsp-cre;Pten^{loxP/loxP}* (n=26) donors were transplanted into syngeneic wild-type recipients and tumor development was monitored over the course of several months¹⁹. By genetically marking the stroma with the *Rosa26^{LoxP}* reporter allele, we could show that both the epithelium and its associated stroma were effectively transplanted into host female mice (Supplementary Fig. 4). By 16 weeks post-transplantation, loss of *Pten* in stromal fibroblasts dramatically increased the incidence of *ErbB2*-driven mammary tumors (Fig. 2b). By 26 weeks most of these females met the criteria for early removal due to excessive tumor burden, whereas few control *ErbB2* females had palpable tumors (Fig. 2a-d). Stromal deletion of *Pten* also dramatically accelerated development of *MYC* mammary tumors (Fig. 2e-g). By 16 weeks post-transplantation, most of these lesions progressed to adenoma, carcinoma *in situ* and invasive carcinoma (Fig. 2h). Histological examination showed that *ErbB2*- and *MYC*-tumor cells in *Pten* stromal-deleted tumors retained their typical oncogene-specific morphology. *ErbB2*-cells had small nuclei, fine

chromatin and abundant eosinophilic cytoplasm¹⁹, whereas *MYC*-tumor cells had pleomorphic nuclei with coarse chromatin and amphophilic cytoplasm. In contrast to non-deleted tumors, which typically had relatively little stromal contribution^{19, 20}, *Pten* stromal-deleted tumors had a significant amount of stroma surrounding and infiltrating the epithelial masses (Fig. 2d, 2h). PCR-based and immunohistochemical assays confirmed that all tumors had an intact *Pten*^{loxP} allele in the epithelial compartment (Supplementary Fig. 5a, 5b and data not shown). Thus, the analysis of two distinct breast cancer tumor models identified a potent tumor suppressor role for *Pten* in stromal fibroblasts of the mammary gland.

***Pten* in stromal fibroblasts controls ECM and innate immune functions.**

To investigate the tumor suppressive mechanism of *Pten* action in stromal fibroblasts, we profiled the transcriptome of mammary stromal fibroblasts isolated from *Pten*^{loxP/loxP} (n=3) and *Fsp-cre;Pten*^{loxP/loxP} (n=3) females. Details of sample collection, processing of Affymetrix oligo-arrays and expression data are available in the Methods section. Briefly, we implemented class comparison analyses of all probe sets on the Affymetrix mouse genome 430 2.0 array to identify genes differentially expressed between the two genetic groups. We also used an unbiased approach similar to Gene Set Enrichment Analysis⁹ to identify *a priori* defined groups of genes that were significantly differentially expressed. The analysis of over 14,000 mouse genes identified 129 upregulated and 21 downregulated genes in response to *Pten* deletion (Supplementary Fig. 6a, 6b; >4-fold at p <0.001; Supplementary Tables 1 and 2). Quantitative RT-PCR assays of a subset of genes confirmed >85% of these expression changes using

independent fibroblast samples (Supplementary Fig. 6c, 6d, and Supplementary Table 3) and the lack of macrophage-, endothelial- and epithelial-specific expression confirmed the purity of the fibroblast preparations used for these microarrays (Supplementary Figure 6d). Functional annotation^{21, 22} (GO) of *Pten*-responsive targets revealed a remarkable bias toward genes encoding proteins involved in ECM remodeling, wound healing and inflammation (Fig. 3a). Given this unexpected convergence of function in *Pten* stromal-deleted mammary glands, we performed a more thorough cellular and molecular analysis of *Pten*-deleted stroma. Staining of consecutive mammary gland sections with H&E and Mason's trichrome stains indicated enhanced deposition of collagen in *Pten*-deleted stroma that was independent of *ErbB2*-oncogene expression (Fig. 3b, and Supplementary Fig. 7a). IHC and Western blot assays using collagen type-specific antibodies showed that the non-cellular material consisted mostly of type-I collagen and not the basement membrane type-IV collagen (Fig. 3b, and Supplementary Fig. 7b, 7c). GO analysis also suggested that *Pten* in stromal fibroblasts influenced the expression of a complex network of chemokines, cytokines and receptors known to support chronic inflammation^{21, 22}. Quantification of innate and adaptive immune cells showed significant infiltration of F4/80-positive macrophages into stromal *Pten*-deleted mammary glands (Fig. 3d, 3e), which was also independent of *ErbB2*-oncogene expression (Supplementary Fig. 8). The abundance of B- and T- cells did not change in response to stromal deletion of *Pten* (data not shown). From these experiments we conclude that ablation of *Pten* in stromal fibroblasts recapitulates two key events associated with tumor malignancy: increased ECM deposition and innate immune cell infiltration.

Loss of stromal *Pten* activates an Ets2-dependent transcriptional program

Along with the remarkable remodeling of the tumor microenvironment, loss of *Pten* in stromal fibroblasts resulted in the activation of the Ras, JNK and Akt pathways. Western blot analysis using protein lysates derived from *Pten*-deleted stromal fibroblasts demonstrated an increase in the phospho-specific forms of Akt (T³⁰⁸ and S⁴⁷³) and JNK (T¹⁸³ and Y¹⁸⁵) (Fig 3a). Immunohistochemical assays confirmed the activation of Akt and JNK in stromal fibroblasts, and interestingly, also revealed a profound activation of these two pathways in ductal epithelial cells adjacent to the *Pten*-deleted stroma (Fig. 3g and data not shown). This analysis also showed increased levels of phospho-Erk1/2 in *Pten*-deleted stromal fibroblasts (Fig. 3g), however, this increased could not be detected in primary cultured fibroblasts, presumably due to the constitutive *Pten*-independent activation of Erk1/2 by serum-stimulation²³.

Among the many expression changes observed in *Pten*-deleted stromal fibroblasts we noted that there was a significant increase in *Ets2* mRNA levels (2.8 fold, $p < 0.001$). This induction is notable because the Ets2 transcription factor is known to be transcriptionally induced by MAPK²⁴⁻²⁶ activation and its function to be post-translationally enhanced by the Akt- and JNK-mediated phosphorylation of its pointed domain at threonine 72 (Ets2^{T72})^{23, 27}. Quantitative RT-PCR and Western blot assays confirmed the higher levels of Ets2 mRNA and protein in *Pten*-deleted relative to control fibroblasts (~2.5-fold, $p < 0.001$; Fig. 4a, 4b). Immunofluorescence (IF) assays using vimentin and phospho-specific Ets2^{T72} antibodies revealed a marked increase of P-Ets2^{T72} in stromal fibroblasts and interestingly, in the adjacent epithelial ductwork as well (Fig.

3c, 3d). Loss of *Pten* in stromal fibroblasts resulted in the induction of a number of genes involved in ECM remodeling and macrophage recruitment (Supplementary Fig. 6c), two of which, *Mmp9* and *Ccl3*, are known to be direct transcriptional targets of Ets2^{28, 29} (Fig. 4e). The increase of *Mmp9* expression in *Pten* stromal-deleted *ErbB2*-tumors appears to be of pathological relevance since *in situ* zymography, a functional assay enabling real-time monitoring of a fluorescent protease cleavage substrate³⁰, showed robust activation of Mmp9 in these tumor samples (Fig. 4f). Chromatin immunoprecipitation (ChIP) assays showed an increase in the loading of Ets2 onto the *Mmp9* and *Ccl3* promoters in *Pten*-deleted mammary fibroblasts (Fig. 4g), suggesting a direct role for Ets2 in the transcriptional regulation of these two target genes. Together, these data illustrate the extensive molecular reprogramming that takes place in the tumor microenvironment and in tumor cells, as a consequence of ablating *Pten* in stromal fibroblasts.

Stromal *Ets2* promotes mammary tumorigenesis

To determine whether Ets2 promotes a microenvironment conducive to tumor growth we analyzed the consequences of ablating a conditional allele of *Ets2* (*Ets2*^{loxP})³¹ in mammary stromal fibroblasts of a well-characterized mouse model of breast cancer, *MMTV-PyMT* (*PyMT*)³². The *PyMT* oncogene initiates the rapid onset and progression of mammary tumors and thus represents an ideal model for evaluating any potential delay that loss of *Ets2* might have on tumorigenesis. The complete or near-complete ablation of *Ets2* in stromal fibroblasts was facilitated by using *Fsp-cre* mice carrying conventional and conditional knockout alleles of *Ets2* (DNA-binding domain-*Ets2*^{db/LoxP})³³. PCR-based analysis of genomic DNA showed efficient deletion of *Ets2*^{loxP} in mammary

fibroblasts of *Fsp-cre;Ets2^{db/loxP}* mice (Fig. 5a) and Western blot and IF assays confirmed the loss of its protein product (Fig. 5b and 5c, respectively). Importantly, ablation of *Ets2* in these cells had no detectable physiological consequence on the development of mammary glands, either during puberty or pregnancy (MCO, unpublished observations). The evaluation of *PyMT;Fsp-cre;Ets2^{db/loxP}* and control *PyMT;Ets2^{db/loxP}* mice over a period of three months showed that ablation of *Ets2* in mammary fibroblasts significantly reduced tumorigenesis (Fig. 5d). *PyMT;Fsp-cre;Ets2^{db/loxP}* mice exhibited decreased tumor load (Fig. 5e) and slower progression to adenoma and early carcinoma than *PyMT;Ets2^{db/loxP}* control mice (Fig. 5f). Analysis of *Mmp9* expression by quantitative RT-PCR showed low levels of its mRNA in normal fibroblasts (with or without *Ets2*) and high levels in tumor-associated fibroblasts containing *Ets2*, which were reduced back to the normal low levels upon in *Ets2*-deleted tumor fibroblasts (Fig. 6a). *In situ* zymography assays measured a 4-5 fold decrease in Mmp9 activity in tumor sections from *PyMT;Fsp-cre;Ets2^{db/loxP}* mice relative to *PyMT;Ets2^{db/loxP}* controls (Fig. 6d and data not shown). Because Mmp9 activity is known to mediate the release of matrix-bound VEGF-A to its active isoforms, including VEGF₁₆₄³⁴, we visualized the spatial distribution of VEGF₁₆₄ and Mmp9 by immunofluorescent staining in consecutive frozen tumor sections. These assays showed that the accumulation of VEGF₁₆₄, which was particularly acute within collagen1A-rich stromal locations overlapping Mmp9 activity, was significantly decreased in stromal-deleted *Ets2* tumors (Fig. 6b, 6d). Given that VEGF₁₆₄ is a specific ligand for VEGF Receptor 2 (VEGFR2; FLK-1; KDR), one of the most potent mediators of VEGF-induced endothelial signaling and angiogenesis³⁵, we also evaluated VEGFR2 status by immuno-staining tumor sections with antibodies

specific for CD31 (endothelial-specific marker) and the phospho-activated form of the murine VEGF receptor (VEGFR2^{Y1173})³⁶. This analysis revealed a four-fold decrease in the number of CD31/ VEGFR2^{Y1173} double-positive cells in *Ets2*-deleted versus non-deleted tumor samples (Fig. 6c, 6e). Together, we conclude that loss of *Ets2* in stromal fibroblasts resulted in decreased *Mmp9* expression and activity in the tumor ECM and reduced VEGFR2^{Y1173}-activation in the tumor vasculature.

Loss of *Ets2* diminishes tumor formation in *Pten* stromal-deleted mammary glands

Given the apparent role of stromal *Ets2* in promoting *PyMT*-driven mammary tumors, we entertained the hypothesis that *Ets2* may be contributing to the remodeling of the tumor microenvironment caused by stromal *Pten* deletion that led to enhanced tumorigenesis in *ErbB2;Fsp-cre;Pten^{loxP/loxP}* mice. To directly test this possibility, we compared tumor incidence and burden in *Pten^{loxP/loxP}*, *Fsp-cre;Pten^{loxP/loxP}* and *Fsp-cre;Pten^{loxP/loxP}Ets2^{db/loxP}* mammary glands that were orthotopically injected with an established *ErbB2*-initiated mammary tumor cell line (NT 2.5)³⁷. This orthotopic model recapitulated the consequences of deleting *Pten* in the mammary stroma that were observed in the genetically engineered *ErbB2*-mouse model described earlier in this study. Indeed, the incidence of tumors at injected sites and the tumor load in *Fsp-cre;Pten^{loxP/loxP}* females was markedly higher than in control *Pten^{loxP/loxP}* females (Fig. 7a, 7b). Importantly, both the tumor incidence and tumor loads were significantly reduced in mammary glands doubly deleted for stromal *Pten* and *Ets2* (*Fsp-cre;Pten^{loxP/loxP}Ets2^{db/loxP}*). Evaluation of tumor sections revealed decreased number of macrophages and recruitment of new vasculature in these doubly-deleted mammary

glands (Fig. 7d, 7e). Loss of *Pten* and *Ets2*, however, failed to fully reduce the tumor load and the excessive collagen deposition to control levels (compare *Pten*^{loxP/loxP} and *Fsp-cre;Pten*^{loxP/loxP};*Ets2*^{db/loxP} in Fig. 7b, 7d and 7e), suggesting that additional effectors must also contribute towards Pten's tumor suppressor functions. From these data, we conclude that *Ets2* is a major component of the Pten tumor suppressive axis that acts in the stromal fibroblast compartment of mammary glands.

Mouse fibroblast Pten expression signature distinguishes normal from tumor stroma in breast cancer patients.

To determine the relevance of these findings in mice to human breast cancer, we compared the stromal fibroblast Pten-expression signature identified in *Fsp-cre;Pten*^{loxP/loxP} mice to the expression signatures derived from laser-captured tumor stroma (49 samples) and adjacent normal stroma (52 samples) in breast cancer patients³⁸. Details of sample processing and data analysis are available in the Supplementary Methods section. First, we identified 137 human orthologs from the 150 differentially expressed mouse genes detected by the Affymetrix oligo-arrays (Supplementary Fig. 6). Of these 137 orthologs, 129 genes were represented in the expression platform used³⁸ (Agilent) for the analysis of human patient stroma samples (McGill Cancer Center's Breast Stroma Microarray data GSE9014 and GSE4823). Only 71 of these 129 genes had highly variable gene expression across all human stromal samples (a variance cutoff of >0.5). The heat map generated for the human stroma dataset showed that this 71 gene-subset derived from the mouse Pten-signature was sufficient to distinguish normal from tumor stroma in all patients (Fig. 8a; $p=3.9e^{-15}$ as determined by Wilcoxon's test).

Interestingly, 12 of the 137 human orthologs identified by the *Pten*-signature (Fig. 8a, highlighted in red) were previously shown to be differentially expressed in the tumor stroma of breast cancer patients and to be associated with recurrence³⁸. This overlap between differentially expressed genes in mouse (71 genes) and human stroma (163 genes) is highly significant ($p = 2.5e-8$, Fisher's Exact Analysis). These analyses suggest that the fibroblast *Pten*-expression signature identified by our stroma mouse model represents a significant subset of the total gene signature expressed in the stroma of human breast cancer. We interpret these results to mean that a portion of the transcriptome regulated by *Pten* in mammary stromal fibroblasts is dysregulated in the tumor stroma of breast cancer patients.

DISCUSSION

Histopathology and molecular studies suggest that malignant tumors consist of a complex cellular system that is dependent on reciprocal signaling between tumor cells and the adjacent stroma. However, the signaling pathways that mediate the communication between the various cell types in the tumor remain virtually unknown. We recently developed a mesenchymal-specific *cre* mouse¹⁵ and used it here to examine the consequences of inactivating *Pten* in mammary stromal fibroblasts. Using this system we show, for the first time, that *Pten* in stromal fibroblasts has a critical role in the suppression of epithelial mammary tumors that is, in part, mediated through an *Ets2*-regulated transcriptional program.

The tumor suppressor functions of *PTEN* have been extensively studied in the tumor cell³⁹⁻⁴¹. We show here that genetic ablation of *Pten* in mammary stromal

fibroblasts of mice alters the expression profile of these cells to increase ECM, chemokine and cytokine production in the tumor microenvironment. As a result, *Pten* stromal-deleted tumors exhibit high levels of collagen, macrophage recruitment and vascular networks, which together favor the initiation and progression of mammary epithelial tumors. Remarkably, side-by-side evaluation of histopathology by independent pathologists could not distinguish tumors between *Pten* stromal-deleted mice and human breast cancer patients, highlighting the importance of modeling stromal cell compartments of the tumor microenvironment. The mechanism by which *Pten* in the stroma exerts its tumor suppressor role likely involves the control of multiple signaling pathways, including components of the Ras, Akt and JNK networks, which together culminate in the regulation of Ets2 transcriptional activity. The fact that loss of *Ets2* in mammary stromal fibroblasts diminished the oncogenic consequences of deleting *Pten* in these cells underscores the importance of the stromal Pten-Ets2 axis in stromal fibroblasts during tumor suppression. These observations are consistent with previous work from Oshima and colleagues that showed a critical cell non-autonomous role for *Ets2* in the growth of mammary tumors in mice⁴² and with the identification of Ets2 activation as a key event associated with breast cancer in human patients having poor prognosis⁴³⁻⁴⁵. The relevance of the mouse Pten-Ets2 tumor suppression axis identified here to human breast cancer is highlighted by the high correspondence between the mouse and human stromal expression signatures. The observation that the dire consequences of targeting this *Ets2*-driven stromal program are tumor-specific, sparing normal mammary development, emphasizes the potential utility of stromal-specific strategies for therapeutic intervention in human breast cancer.

In summary, this work identifies *Pten-Ets2* as a key regulatory axis in stromal fibroblasts that suppresses mammary epithelial tumors by profoundly attenuating some of the most malignant characteristics of the tumor microenvironment. This novel function of *Pten* may be relevant in the suppression of epithelial tumors of other organs, but may also extend beyond cancer, to conditions where the microenvironment may impact disease manifestation, such as in autoimmune syndromes⁴⁶, lung fibrosis⁴⁷ and neurodegeneration⁴⁸. Interestingly, the stromal *Pten* expression signature identified here includes genes that have been causally linked to ECM deposition and inflammation in rheumatoid arthritis, lung fibrosis and neurodegeneration (Listed in Supplementary Table1 and Table 2). These data offers a molecular basis for how altered *Pten* signaling in the tumor stroma may elicit broad responses in a variety of cells in the tumor microenvironment that contribute to disease manifestation.

ACKNOWLEDGEMENTS

The authors thank Maysoon Rawahneh and Julie Moffitt for excellent histotechnical assistance, Karl Kornacker for bioinformatics assistance, the OSUCCC Microarray, Nucleic Acids, Trangenics and Flow Cytometry Shared Facilities for technical assistance. *MMTV-rtTA* and *MMTV-ErbB2* mice were kindly provided by Dr. Chodosh and Dr. Muller, respectively. This work was funded by the National Institutes of Health to G.L. (R01CA85619, R01HD47470, P01CA097189) and to M.C.O. (P01CA097189), to F.L. by a Department of Defense Pre-doctoral Fellowship. G.L. is the recipient of the Pew Charitable Trusts Scholar Award and the Leukemia and Lymphoma Society Scholar Award. MP holds the Diane and Sal Guerrero Chair in Cancer Genetics at McGill University. Funding for this research provided by Terry Fox New Frontiers Group Grant to MP. Natural Science and Engineering Research Council of Canada Discovery Grants Program grant to M.H.; a US Department of Defense Breast Cancer Predoctoral Traineeship Award to F.P.; M.P. holds the Diane and Sal Guerrero Chair in Cancer Genetics at McGill University. Sean Cory and Indrani Vasudeva Murthy as they ran many of the analyses for us.

METHODS SUMMARY

Transgenic mice. Generation of *Fsp-cre* mice has been described¹⁵. *Pten*^{loxP} mice were created following the strategy described in Supplementary Fig. S1. *Ets2*^{loxP} mice were generated by standard techniques³¹. Animals were maintained and euthanized following institutional guidelines. Tenth generation congenic (N10) FVB/N animals were used for transplantation and orthotopic injection studies.

Tissue processing, histology. All tissues were either fixed with 4% PFA and embedded in OCT, or fixed with formalin and embedded in paraffin. Frozen sections were used for X-gal staining as described¹⁵. To perform gelatinase *in situ* zymography 10µm frozen sections were incubated with 40 ug/ml DQ-gelatin (Molecular Probes) for 10hours at room temperature as described by Mook *et al*⁴⁹.

Isolation of primary mammary fibroblasts. Primary mammary fibroblasts were purified following the protocol published previously with minor modifications⁵⁰. Mammary glands were dissected from 8 week-old female mice, minced and digested with collagenase (0.15% Collagenase I, 160 U/ml Hyaluronidase, 1 ug/ml hydrocortisone and 10 ug/ml insulin with penicillin and streptomycin) in a 5% CO2 incubator overnight at 37°C. Collagenase was neutralized with 10% FBS-DMEM medium. Digested tissue was resuspended in medium and subjected to gravity for 12-15 min. Pellets were washed three times to collect epithelial organoids, and supernatants were subjected four more times to gravity and then cultured.

RNA and microarray analysis. RNA was harvested with Trizol according to manufacturer's instructions (Invitrogen). RNA quality and concentration were assessed by Bioanalyzer and Nanodrop RNA 6000 nano-assay. RNA samples were hybridized to Affymetrix GeneChip Mouse genome 430 2.0 platform at the Microarray Shared Resource Facility, Ohio State University Comprehensive Cancer Center.

REFERENCES

1. Wiseman, B. S. & Werb, Z. Stromal effects on mammary gland development and breast cancer. *Science* 296, 1046-9 (2002).
2. Nelson, C. M. & Bissell, M. J. Of extracellular matrix, scaffolds, and signaling: tissue architecture regulates development, homeostasis, and cancer. *Annu Rev Cell Dev Biol* 22, 287-309 (2006).
3. Mueller, M. M. & Fusenig, N. E. Friends or foes - bipolar effects of the tumour stroma in cancer. *Nat Rev Cancer* 4, 839-49 (2004).
4. Schedin, P. Pregnancy-associated breast cancer and metastasis. *Nat Rev Cancer* 6, 281-91 (2006).
5. Littlepage, L. E., Egeblad, M. & Werb, Z. Coevolution of cancer and stromal cellular responses. *Cancer Cell* 7, 499-500 (2005).
6. Bhowmick, N. A., Neilson, E. G. & Moses, H. L. Stromal fibroblasts in cancer initiation and progression. *Nature* 432, 332-7 (2004).
7. Kalluri, R. & Zeisberg, M. Fibroblasts in cancer. *Nat Rev Cancer* 6, 392-401 (2006).
8. Cully, M., You, H., Levine, A. J. & Mak, T. W. Beyond PTEN mutations: the PI3K pathway as an integrator of multiple inputs during tumorigenesis. *Nat Rev Cancer* 6, 184-92 (2006).
9. Bergamaschi, A. et al. Extracellular matrix signature identifies breast cancer subgroups with different clinical outcome. *J Pathol* 214, 357-67 (2008).
10. Myers, M. P. et al. The lipid phosphatase activity of PTEN is critical for its tumor suppressor function. *Proc Natl Acad Sci U S A* 95, 13513-8 (1998).
11. Stambolic, V. et al. Negative regulation of PKB/Akt-dependent cell survival by the tumor suppressor PTEN. *Cell* 95, 29-39 (1998).
12. Salmena, L., Carracedo, A. & Pandolfi, P. P. Tenets of PTEN tumor suppression. *Cell* 133, 403-14 (2008).
13. Knobbe, C. B., Lapin, V., Suzuki, A. & Mak, T. W. The roles of PTEN in development, physiology and tumorigenesis in mouse models: a tissue-by-tissue survey. *Oncogene* 27, 5398-415 (2008).
14. Di Cristofano, A., Pesce, B., Cordon-Cardo, C. & Pandolfi, P. P. Pten is essential for embryonic development and tumour suppression. *Nat Genet* 19, 348-55 (1998).
15. Trimboli, A. J. et al. Direct evidence for epithelial-mesenchymal transitions in breast cancer. *Cancer Res* 68, 937-45 (2008).
16. Guy, C. T. et al. Expression of the neu protooncogene in the mammary epithelium of transgenic mice induces metastatic disease. *Proc Natl Acad Sci U S A* 89, 10578-82 (1992).
17. D'Cruz, C. M. et al. c-MYC induces mammary tumorigenesis by means of a preferred pathway involving spontaneous Kras2 mutations. *Nat Med* 7, 235-9 (2001).
18. Gunther, E. J. et al. A novel doxycycline-inducible system for the transgenic analysis of mammary gland biology. *FASEB J* 16, 283-92 (2002).
19. Cases S, et al. Development of the mammary gland requires DGAT1 expression in stromal and epithelial tissues. *Development* 131, 3047-55. (2004).

19. Andrechek, E. R. et al. Amplification of the neu/erbB-2 oncogene in a mouse model of mammary tumorigenesis. *Proc Natl Acad Sci U S A* 97, 3444-9 (2000).
20. Desai, K. V. et al. Initiating oncogenic event determines gene-expression patterns of human breast cancer models. *Proc Natl Acad Sci U S A* 99, 6967-72 (2002).
21. Dennis, G., Jr. et al. DAVID: Database for Annotation, Visualization, and Integrated Discovery. *Genome Biol* 4, P3 (2003).
22. Huang da, W., Sherman, B. T. & Lempicki, R. A. Systematic and integrative analysis of large gene lists using DAVID bioinformatics resources. *Nat Protoc* 4, 44-57 (2009).
23. Weng, L. P., Brown, J. L., Baker, K. M., Ostrowski, M. C. & Eng, C. PTEN blocks insulin-mediated ETS-2 phosphorylation through MAP kinase, independently of the phosphoinositide 3-kinase pathway. *Hum Mol Genet* 11, 1687-96 (2002).
24. Chung, J. H. et al. The ERK1/2 pathway modulates nuclear PTEN-mediated cell cycle arrest by cyclin D1 transcriptional regulation. *Hum Mol Genet* 15, 2553-9 (2006).
25. Fowles, L. F. et al. Persistent activation of mitogen-activated protein kinases p42 and p44 and ets-2 phosphorylation in response to colony-stimulating factor 1/c-fms signaling. *Mol Cell Biol* 18, 5148-56 (1998).
26. McCarthy, S. A. et al. Rapid phosphorylation of Ets-2 accompanies mitogen-activated protein kinase activation and the induction of heparin-binding epidermal growth factor gene expression by oncogenic Raf-1. *Mol Cell Biol* 17, 2401-12 (1997).
27. Smith, J. L. et al. ets-2 is a target for an akt (Protein kinase B)/jun N-terminal kinase signaling pathway in macrophages of motheaten-viable mutant mice. *Mol Cell Biol* 20, 8026-34 (2000).
28. Watabe, T. et al. The Ets-1 and Ets-2 transcription factors activate the promoters for invasion-associated urokinase and collagenase genes in response to epidermal growth factor. *Int J Cancer* 77, 128-37 (1998).
29. Wei, G. et al. Activated Ets2 is required for persistent inflammatory responses in the motheaten viable model. *J Immunol* 173, 1374-9 (2004).
30. Ludwig, T. Local proteolytic activity in tumor cell invasion and metastasis. *Bioessays* 27, 1181-91 (2005).
31. Wei, G. et al. Ets1 and Ets2 are required for endothelial cell survival during embryonic angiogenesis. *Blood* (2009).
32. Lin, E. Y. et al. Progression to malignancy in the polyoma middle T oncoprotein mouse breast cancer model provides a reliable model for human diseases. *Am J Pathol* 163, 2113-26 (2003).
33. Yamamoto, H. et al. Defective trophoblast function in mice with a targeted mutation of Ets2. *Genes Dev* 12, 1315-26 (1998).
34. Lee, S., Jilani, S. M., Nikolova, G. V., Carpizo, D. & Iruela-Arispe, M. L. Processing of VEGF-A by matrix metalloproteinases regulates bioavailability and vascular patterning in tumors. *J Cell Biol* 169, 681-91 (2005).

35. Millauer, B. et al. High affinity VEGF binding and developmental expression suggest Flk-1 as a major regulator of vasculogenesis and angiogenesis. *Cell* 72, 835-46 (1993).
36. Sakurai, Y., Ohgimoto, K., Kataoka, Y., Yoshida, N. & Shibuya, M. Essential role of Flk-1 (VEGF receptor 2) tyrosine residue 1173 in vasculogenesis in mice. *Proc Natl Acad Sci U S A* 102, 1076-81 (2005).
37. Dakappagari, N. K. et al. Conformational HER-2/neu B-cell epitope peptide vaccine designed to incorporate two native disulfide bonds enhances tumor cell binding and antitumor activities. *J Biol Chem* 280, 54-63 (2005).
38. Finak, G. et al. Stromal gene expression predicts clinical outcome in breast cancer. *Nat Med* 14, 518-27 (2008).
39. Berns, K. et al. A functional genetic approach identifies the PI3K pathway as a major determinant of trastuzumab resistance in breast cancer. *Cancer Cell* 12, 395-402 (2007).
40. Saal, L. H. et al. Recurrent gross mutations of the PTEN tumor suppressor gene in breast cancers with deficient DSB repair. *Nat Genet* 40, 102-7 (2008).
41. Saal, L. H. et al. Poor prognosis in carcinoma is associated with a gene expression signature of aberrant PTEN tumor suppressor pathway activity. *Proc Natl Acad Sci U S A* 104, 7564-9 (2007).
42. Tynan, J. A., Wen, F., Muller, W. J. & Oshima, R. G. Ets2-dependent microenvironmental support of mouse mammary tumors. *Oncogene* 24, 6870-6 (2005).
43. Buggy, Y. et al. Ets2 transcription factor in normal and neoplastic human breast tissue. *Eur J Cancer* 42, 485-91 (2006).
44. Park, E. S. et al. Heterologous tissue culture expression signature predicts human breast cancer prognosis. *PLoS ONE* 2, e145 (2007).
45. Svensson, S. et al. ERK phosphorylation is linked to VEGFR2 expression and Ets-2 phosphorylation in breast cancer and is associated with tamoxifen treatment resistance and small tumours with good prognosis. *Oncogene* 24, 4370-9 (2005).
46. Pap, T. et al. Activation of synovial fibroblasts in rheumatoid arthritis: lack of Expression of the tumour suppressor PTEN at sites of invasive growth and destruction. *Arthritis Res* 2, 59-64 (2000).
47. White, E. S. et al. Negative regulation of myofibroblast differentiation by PTEN (Phosphatase and Tensin Homolog Deleted on chromosome 10). *Am J Respir Crit Care Med* 173, 112-21 (2006).
48. Gibson, G. E. & Huang, H. M. Oxidative processes in the brain and non-neuronal tissues as biomarkers of Alzheimer's disease. *Front Biosci* 7, d1007-15 (2002).
49. Mook, O. R., Van Overbeek, C., Ackema, E. G., Van Maldegem, F. & Frederiks, W. M. In situ localization of gelatinolytic activity in the extracellular matrix of metastases of colon cancer in rat liver using quenched fluorogenic DQ-gelatin. *J Histochem Cytochem* 51, 821-9 (2003).
50. Soule, H. D. & McGrath, C. M. A simplified method for passage and long-term growth of human mammary epithelial cells. *In Vitro Cell Dev Biol* 22, 6-12 (1986).

FIGURE LEGENDS

Figure 1 Stromal fibroblast-specific deletion of *Pten*.

(a) *Fsp-cre* expression in the mammary gland. Whole mount X-gal stained mammary glands from *Fsp-cre;Rosa^{+/-loxP}* and *Rosa^{+/-loxP}* (top inset) mice. Higher magnification micrograph of whole mount (bottom left) and cross section (bottom right) of *Fsp-cre;Rosa^{+/-loxP}* X-gal stained mammary gland; lu, lumen.

(b) *Pten* deletion in the *Fsp-cre;Pten^{loxP/loxP}* mice by PCR-based assays. DNA extracted from tail biopsies (lanes 1-4) or purified primary mammary stromal fibroblasts (lanes 5-7) with the indicated genotypes were used as template for PCR-based measurement of *Pten* deletion using primers described in Methods.

(c) Ablation of *Pten* protein in mammary stromal fibroblasts. Representative Western blot analysis of mammary fibroblast lysates derived from four different 8 week-old female mice with the indicated genotypes.

(d) *Pten* inactivation is restricted to mammary stromal fibroblasts. Paraffin sections from *Pten^{loxP/loxP}* and *Fsp-cre;Pten^{loxP/loxP}* mammary glands were processed for IHC using a *Pten*-specific antibody. Lower panels represent higher magnification of boxed areas in upper panels. lu, lumen; epi, epithelial compartment; str, stromal compartment; red dotted line indicates the border between the epithelial and stromal compartments.

Figure 2 Loss of *Pten* in mammary stromal fibroblasts accelerates tumorigenesis.

- (a) Tumors derived from *ErbB2;Pten^{loxP/loxP}* and *ErbB2;Fsp-cre;Pten^{loxP/loxP}* mammary glands, 26 weeks post-transplantation.
- (b) Percentage of mammary glands with the indicated genotypes that developed tumors by 16 weeks post-transplantation. Tumorigenicity was determined based on palpation or histological presentation of adenoma/carcinoma at each implantation site and statistically analyzed using Fisher's Exact test.
- (c) Total tumor burden in mammary glands with the indicated genotypes at 26 weeks post-transplantation. A mixed ANOVA model was used to compare the groups. A random effect for the mouse within donor effect was used to account for the correlations.
- (d) H&E stained sections of mammary glands with the indicated genotypes that were harvested just before transplantation (0 weeks) and at the indicated times post-transplantation.
- (e) Tumors derived from *MYC;Pten^{loxP/loxP}* and *MYC;Fsp-cre;Pten^{loxP/loxP}* mammary glands, 10 weeks post-transplantation.
- (f) Percentage of mammary glands with the indicated genotypes that developed tumors by 10 weeks post-transplantation. Tumorigenicity was determined based on histological presentation of adenoma/carcinoma at each implantation site. Note that no tumors developed in *MYC;Pten^{loxP/loxP}* mammary glands and hence no statistical analysis was performed.
- (g) Total tumor burden in mammary glands with the indicated genotypes at 26 weeks post-transplantation. A mixed ANOVA model was used to compare the groups. A random effect for the mouse within donor effect was used to account for the correlations.

(h) Paraffin sections of mammary glands with the indicated genotypes were harvested at 10 weeks post-transplantation and stained with H&E. Note the range of tumor stage observed in *MYC;Fsp-cre;Pten^{loxP/loxP}* glands.

Figure 3 Characterization of ECM deposition and immune cell infiltration.

- (a) Schematic representation of the biological processes affected by differentially expressed genes (<4 fold).
- (b) Tissue sections from 8 week-old *Pten*^{loxP/loxP} and *Fsp-cre;Pten*^{loxP/loxP} mammary glands were stained with H&E, Masson's Trichrome and Collagen I-specific antibodies, respectively.
- (c) Quantification of collagen deposition (trichrome-positive area) in mammary glands with the indicated genotypes. Trichrome-stained sections were imaged using an Aperio Scanscope CS whole-slide scanner. Areas of skin and muscle, which also stain positive, were manually encircled and excluded from the analysis. Values shown represent the mean with standard deviation; Wilcoxon Rank Sum test was used for the comparison between groups.
- (d) Sections from mammary glands with the indicated genotypes were stained with the macrophage-specific marker F4/80.
- (e) Quantification of stromal cells stained positive for the macrophage-specific marker F4/80 in mammary glands with the indicated genotypes. Values shown represent the mean with standard deviation; Wilcoxon Rank Sum test was used for the comparison between groups.
- (f) Western blot analysis of whole-cell lysates derived from stromal fibroblasts with the indicated genotypes and antibodies; blots were probed with anti-tubulin as a loading control.
- (g) Sections from mammary glands with the indicated genotypes stained with the phospho-Akt^{473/308}, phospho-JNK^{183/185}, and phospho-Erk1/2 specific antibodies.

Figure 4 Loss of *Pten* in stromal fibroblasts leads to activation of Ets2.

(a) qRT-PCR analysis of *Ets2* expression in *Pten*^{loxP/loxP} and *Fsp-cre;Pten*^{loxP/loxP} stromal fibroblasts. Total RNA was isolated from fibroblasts with the indicated genotypes and analyzed by real-time RT-PCR assays. Values shown represent the average with standard deviation; statistical analysis used the Student t-test.

(b) Western blot analysis of whole-cell lysates derived from fibroblasts with the indicated genotypes.

(c) Quantification of (Fig 4d) mammary epithelial and stromal cells that stain positive for nuclear phospho-Ets2^{T72} in *Pten*^{loxP/loxP} and *Fsp-cre;Pten*^{loxP/loxP} animals. Values shown represent the mean with standard deviation; Wilcoxon Rank Sum test was used for the statistical comparison between groups.

(d) Mammary tissue sections from *Pten*^{loxP/loxP} and *Fsp-cre;Pten*^{loxP/loxP} animals were processed for IF using a phospho-Ets2^{T72}-specific antibody. Note that loss of *Pten* in the mammary stroma increased Ets2 phosphorylation in both the stromal and epithelial compartments. Dotted-white line indicates the stromal-epithelial boundary.

(e) qRT-PCR analysis of *Mmp9* expression in *Pten*^{loxP/loxP} and *Fsp-cre;Pten*^{loxP/loxP} stromal fibroblasts. Total RNA was isolated from fibroblasts with the indicated genotypes and analyzed by real-time RT-PCR assays. Values shown represent the average with standard deviation; statistical analysis used the Student t-test. Note that *Mmp9* expression is increased in *Pten*-deleted fibroblasts and further increased in *Pten*-deleted fibroblasts derived from mammary glands expressing *ErbB2* in the epithelial compartment.

(f) *In situ* zymogen IF assays in 26 week post-transplanted *ErbB2;Pten^{loxP/loxP}* and *ErbB2;Fsp-cre;Pten^{loxP/loxP}* mammary glands (bottom panels). Top panels are H&E staining of consecutive sections from the same mammary gland in bottom panels.

(g) ChIP assays using Ets2-specific or IgG control antibodies in stromal fibroblasts with the indicated genotypes. Values shown represent the average with standard deviation; statistical analysis used the Student t-test.

Figure 5 Ets2 ablation in stroma fibroblasts restricts mammary tumorigenesis.

- (a) Ets2 genotyping and (b) Western blot of fibroblasts purified from mammary glands of *PyMT;Ets2^{db/loxP}* (lane 1) or *PyMT;Fsp-Cre;Ets2^{db/loxP}* mice (lane2).
- (c) Immunofluorescence staining of cultured mammary fibroblasts from 9 week-old mice with Vimentin (green) and p-Ets2(T⁷²) (red) antibodies, and counterstained with DAPI. Scale bar is 50µm.
- (d) Representative images of gross tumors dissected four weeks post tumor initiation from *PyMT;Ets2^{db/loxP}* (left) or *PyMT;Fsp-cre;Ets2^{db/loxP}* (right) mice.
- (e) Comparison of total mammary tumor volume of *PyMT;Ets2^{db/loxP}* (n = 20), *PyMT;Fsp-cre;Ets2^{db/loxP}* (n = 21) mice; significance based on Wilcoxon Rank Sum test.
- (f) H&E staining of tumors harvested from *PyMT;Ets2^{db/loxP}* or *PyMT;Fsp-cre;Ets2^{db/loxP}* mice; Scale bar is 500µm for top panel and 50µm for bottom panel.

Figure 6 Ets2 inactivation in tumor fibroblasts impairs vascular endothelial signaling and reduces tumor angiogenesis

- (a) Quantitative RT-PCR analysis of *Mmp9* mRNA expression in primary mammary fibroblasts of indicated genotypes (* $P < 0.01$, $n = 3$, Students t-test).
- (b) Quantification of VEGF₁₆₄ of the IF staining (Fig 6d) in tumor stroma area in tumors collected one week post tumor initiation(* $P < 0.01$, $n = 3$, Students T-test). Error bars represent s.d.
- (c) Quantification of tumor endothelial cells (Fig 6e) co-expressing CD31 and phospho-VEGFR2 (* $P < 0.01$, $n = 3$, Student T-test).
- (d) Consecutive sections stained for (from left to right): Trichrome, Mmp9 gelatinase activity and VEGF₁₆₄, and counterstained with DAPI from *PyMT;Ets2^{db/loxP}* and *PyMT;Fsp-cre;Ets2^{db/loxP}* mammary tumors harvested one week post tumor initiation. Scale bars are 50 μ m.
- (e) Tumor vascular endothelial cells visualized by IF double staining with CD31 (green) and p-VEGFR2(Tyr1173) (red), and counterstained with DAPI in mammary tumors collected one week post tumor initiation *PyMT;Ets2^{db/loxP}* and *PyMT;Fsp-cre;Ets2^{db/loxP}* mice. Scale bars are 50 μ m.

Figure 7 Loss of *Ets2* in stromal fibroblasts diminishes tumor growth in stromal *Pten*-deleted mammary glands.

(a) Orthotopic injection of the *ErbB2*-expressing tumor cell line NT 2.5 into *Pten*^{loxP/loxP};*Ets2*^{db/loxP};*Pten*^{loxP/loxP} and *Fsp-cre*;*Pten*^{loxP/loxP} and *Fsp-cre*;*Ets2*^{db/loxP};*Pten*^{loxP/loxP} mammary glands. Mammary glands from at one month post-injection were sectioned and stained with H&E.

(b) The *Pten*^{loxP/loxP};*Ets2*^{db/loxP} (n=10) and *Pten*^{loxP/loxP} (n=10) control groups were combined (+(*), n=20) after it was determined there was no statistical difference in the tumor incidence/load between these two control groups. Values shown represent the mean with standard deviation; Wilcoxon Rank Sum test was used for the comparison between groups.

(c) Sections from mammary glands with the indicated genotypes stained with the macrophage-specific marker F4/80. Frozen sections from 8 week-old mammary tissue with the indicated genotypes stained with the endothelial-specific antibody, CD31, and H&E (consecutive section). Note that loss of *Pten* in the mammary stroma resulted in a disruption of the normal vascular architecture.

(d) Quantification of stromal cells stained positive for the macrophage-specific marker F4/80 in mammary glands with the indicated genotypes. Values shown represent the mean with standard deviation; Wilcoxon Rank Sum test was used for the comparison between groups.

(e) Quantification of collagen deposition (trichrome-positive area) in mammary glands with the indicated genotypes. Trichrome-stained sections were imaged using an Aperio Scanscope CS whole-slide scanner. Areas of skin and muscle, which also stain positive,

were manually encircled and excluded from the analysis. Values shown represent the mean with standard deviation; Wilcoxon Rank Sum test was used for the comparison between groups.

Figure 8 Analysis of the PTEN null mouse fibroblast microarray data.

(a) Heat map comparing 71 human orthologs from the PTEN null fibroblast list, both up- and down-regulated (y-axis), with the genes that are differentially expressed in human tumor stroma from the McGill study. Red and green regions indicate up-regulate and down-regulated genes, respectively, between the normal and tumor stroma sets from human patients.

(b) Gene expression changes assessed by qRT-PCR to confirm microarray results for representative genes that are differentially expressed between fibroblasts with and without *Pten*. Gene expression was analyzed in independent experiments and the averages between duplicates are shown with standard deviation.

(c) Venn diagram depicting the overlap between the mouse *Pten*-deleted fibroblast and human stroma microarray data. This overlap is highly significant (p-value=2.5e-8; Fisher's Exact Analysis).

SUPPLEMENTARY METHODS

Transgenic mice. Animals were housed according to federal and OSU ULAR regulations.

***Fsp-cre*.** The generation of the *Fsp-cre* mouse line has been previously described¹.

***Ets2^{loxP}*.** The *Ets2* conditional transgenic mouse line was generated such that the *Ets2* pointed domain is “floxed”². The pointed domain is encoded by exons 3-5 and important for the protein-protein interaction and signal transduction.

***Ets2^{db}*.** *Ets2^{db}* mouse was a gift from Dr. Oshima R.G. (Burnham Institute for Medical Research, La Jolla, California).

***Pten^{loxP}*.** *LoxP* sites were introduced into two *HpaI* sites within introns 3 and 5 of the *Pten* gene, respectively, to flank exons 4 and 5. Exon 5 encodes the lipid phosphatase domain. Tissue-specific expression of *cre* will excise exons 4 and 5, generating a loss-of-function *Pten^Δ* allele (Supplementary Figure 1; G.W. and M.C.O. unpublished data.). A list of PCR primers can be found on Supplementary Table 3.

Mammary tissue transplantation. Transplant procedure was based on a previously method³. The day prior to surgery, recipient mice were anesthetized with Isoflurane (Abbott Laboratories) and a 25mm x 25mm square area along the scapular region was shaved. At the time of surgery, inguinal and groin mammary tissue (5x5mm in size; minus lymph node) was removed from eight to nine-week-old donor females and placed subcutaneously into the scapular region of wild-type hosts through two 5-10mm incisions on the left and right side under aseptic conditions. The small incisions were closed using

a 9mm wound clip. Animals were monitored twice a week until tumor onset. Mice were sacrificed either at specific time points, when the tumor was about 2 cm in size or it presented a health problem to the animal such as exterior ulceration at the site of the tumor. The *myc* tumor model is an inducible system⁴, but donor mice were never given doxycycline. Instead, recipient mice were started on chow containing doxycycline (1g/kg) prior to the transplant procedure, and then continued until the end of the 10 week study.

Orthotopic mammary gland injection. The neu-expressing mouse mammary carcinoma cell line NT2.5 was provided by Dr. Kaumaya (Ohio State University, Columbus, OH) and was maintained as described⁵. Eight week old female mice of each genotype were anesthetized and injected with 5×10^5 NT2.5 cells at both inguinal mammary glands. Tumor initiation was monitored by palpating twice a week. All the mice were euthanized three weeks after injection. Tumor volume was calculated by formula $V = 1/2 \times \text{length} \times (\text{width})^2$.

Tissue processing and X-gal staining. Large individual tumors (typically ~1 to 2cm) or the remainder of transplanted tissues were removed, divided and either fixed in 4% PFA for 24-48hrs or embedded directly in OCT (Sakura, Torrance, CA). Fixed tissue samples were embedded in paraffin and cut into 5 μm sections for H&E, IHC or IF staining. For each sample collected, two sets of sections were obtained at 25 μm intervals for analysis. Corresponding OCT embedded tissue was sectioned (7 μm) in a similar manner for X-gal or IF staining. For X-gal staining, frozen tissue sections were dried 15 min at RT before fixing in a glutaraldehyde solution (0.2% glutaraldehyde, 1.25mM EGTA, pH 7.3 and

2mM magnesium chloride in 1x PBS) for 30 min. The sections were washed with LacZ wash buffer (2mM magnesium chloride, 0.01% sodium deoxycholate, 0.02% IGEPAL CA-630 (Sigma) in PBS) for 5 min three times and then stained in LacZ staining solution (4 mM potassium ferricyanide, 4mM potassium ferrocyanide, 1mg/mL X-gal in LacZ wash buffer) protected from light at 37°C overnight (~18 hrs). Stained sections were washed in PBS for 5 min three times and then rinsed with water for 2 min before counter-staining with nuclear fast red (NFR). .

Immunohistochemistry and immunofluorescence. IHC or IF was performed using paraffin sections with the following antibodies: Pten (1:100, Cell signaling), Collagen I (1:100, Abcam- 30 min), F4/80 (1:50, Caltag), P-Akt(S473, 1:50, Cell Signaling), P-JNK(1:50, Cell Signaling), P-Erk1/2(1:100, Cell Signaling), P-Ets2(T72, 1:125, M.C.O lab), Cytokeratin 8/18 (1:300; Research Diagnostics- 30 min), E-cadherin (1:700, BD-Pharmingen- 30 min), mouse α -SMA (1:200, Sigma-30 min) and Collagen IV(1:100, Chemicon- 30 min). In general, paraffin sections were deparaffinized and the antigen retrieval accomplished by incubation in antigen retrieval solution (DAKO) at >95°C (30 min). **IHC.** Staining was developed using the biotin/avidin/horseradish peroxidase system from Vector Laboratories according to manufacturer's instructions. All IHC slides were counterstained with hematoxylin and images obtained using an Eclipse 50i microscope (Nikon) and an Axiocam HRc camera (Zeiss). **IF.** Staining was developed using secondary antibodies conjugated to AlexaFluor dyes following standard protocol (Invitrogen; Molecular Probes). For Pten IF the signal was amplified using a biotinylated secondary antibody and Texas Red conjugated to streptavidin. All IF sections were

counterstained with DAPI and images obtained using an Axioscope 40 microscope (Zeiss) equipped with an Axiocam HRc camera (Zeiss). Frozen sections of mammary glands for IF were fixed at 4°C in either 4% paraformaldehyde in PBS or acetone (CD31 and Vimentin). Samples were treated with phospho-Ets2 (T72) (1:125; M.C.O. lab), Vimentin (1:50; Santa Cruz Biotech), VEGF₁₆₄ (1:100, R&D Systems), phospho-VEGFR2Y1175 (1:100, Cell Signaling) and CD31 (1:50, BD Biosciences) antibodies. Fluorescent images were obtained as above. CD31 and phospho-VEGFR2Y1175 images were quantified with software written by Dr. Huang K. VEGF₁₆₄ images were quantified with MetaImaging Series 6.1 software. IHC cells were counted manually and reported as a percentage of positive cells from the total cell population.

Gelatinase *in situ* zymography. This was performed as described, with minor modification¹. Briefly, frozen sections (10um) were quickly fixed with cold acetone, rehydrated with PBS and then incubated with 40 ug/ml DQ-gelatin (Molecular Probes) in reaction buffer (50mM Tris-HCl, 150mM NaCl, 5mM CaCl₂ and 0.2mM NaN₃, PH7.6) for 10hrs. The reaction is quenched with 10mM EDTA-PBS wash. Nuclei are counterstained with DAPI. A consecutive slide is stained with H&E to localize the MMP9 activity.

Western blot. One to two million cells were lysed with RIPA buffer (50mM PH7.4 Tris-HCl, 150mM NaCl, 1mM EDTA, 1% NP-40, 1% Sodium Deoxycholate and 0.1% SDS) containing protease and phosphatase inhibitors (Roche). Primary antibodies for PTEN, Akt, P-Akt, P-JNK, P-Erk, Erk and Ets2 were all used at 1:1000 dilution, while tubulin

was used at 1:5000 dilution. Washed membranes were blotted with either HRP-conjugated anti mouse IgG or anti rabbit IgG antibodies and developed with ECL.

RNA isolation and microarray analysis. Cells were harvested with Trizol and RNA was extracted according to manufacturer's instructions (Invitrogen). Total RNA quality and concentration were assessed by Bioanalyzer and Nanodrop RNA 6000 nano assay. RNA was hybridized to Affymetrix GeneChip, Mouse genome 430 2.0 platform at the Microarray Shared Resource Facility, Ohio State University Comprehensive Cancer Center. The data were analyzed using WEDGE++ expression analysis⁷. Heat map representation (Supplementary Figure 6) was performed using the TIGR Multiexperiment Viewer program [MeV v4.1](#).

Quantitative realtime PCR. Quantitative gene expression was performed using 50 ng cDNA per reaction. Taqman Roche Universal Probe Library system probe and primers (Roche) following manufacturer's instructions. Reactions were carried out on the Icyler iQ Real-Time machine (Bio-Rad).

Chromatin Immunoprecipitation and qPCR. Chromatin immunoprecipitation (ChIP) assays were performed as described by Hu *et al.*⁸ Primary fibroblasts were cross-linked with 1% formaldehyde and soluble chromatin was prepared with sonication to an average DNA length of 200–1000bp. Sheared soluble chromatin was pre-cleared with tRNA-blocked Protein G-agarose, and 10% of the pre-cleared chromatin was set aside as input control. Immunoprecipitation was carried out with 5μg of Ets2 antibody or rabbit IgG

overnight at 4 °C. Immune complexes were pulled down with Protein G-agarose, washed, and eluted with elution buffer (0.1 M NaHCO₃, 1% SDS), and de-crosslinked with 200mM NaCl at 65 °C overnight with 20µg of RNase A (Sigma). DNA was purified with the Qiagen PCR purification kit following proteinase K treatment according to the manufacturer's instructions. Samples were analyzed by real-time PCR as indicated above. The threshold for the promoter being studied was adjusted by that of input values and represented as relative abundance. All qRT-PCR reactions were analyzed by melt curve analysis and agarose gels to confirm the specificity of the reaction.

Generating the Human Stroma Heat map with the fibroblasts - PTEN null genes.

Analysis of the PTEN null mouse microarray data using WEDGE++⁶ led to the identification of 195 differentially expressed probe sets matching to 150 unique mouse genes. A search for human orthologs using Ensembl and MGI databases yielded in a list of 137 genes. These genes were queried against the McGill Cancer Center's Breast Stroma Microarray data (GSE9014 and GSE4823). 129 of the 137 genes were represented on the Agilent Custom Array used in the McGill study. A heat map was generated for the human stroma dataset (52 normal stroma and 49 tumor stroma samples). To achieve better resolution on the heat map, and with the aim of identifying only those genes that had highly variable gene expression across all samples, a variance cutoff of >0.5 was used to generate a subset of 71 genes. The heat map (Figure 8a) shows the ability of these 71 genes to separate the normal and tumor stroma samples based solely on their gene expression profiles. This partitioning is highly significant (p-value=3.9e-

15), as determined by Wilcoxon's test on the average expression of PTEN null-signature in all samples.

Interestingly, comparison of 137 human orthologs of the PTEN null list with the 163 genes associated with recurrence in tumor stroma from the McGill study showed that there are 12 genes (highlighted in red; Fig 8a) present on both gene lists. This overlap is again highly significant (p-value=2.5e-8; Fisher's Exact Analysis).

Statistical Analysis

Animal numbers and experiments are as indicated in the figures. Wilcoxon -rank test was used for most statistical analyses unless mentioned otherwise in the figure legend.

REFERENCES:

1. Trimboli, A. J. et al. Direct evidence for epithelial-mesenchymal transitions in breast cancer. *Cancer Res* 68, 937-45 (2008).
2. Wei, G. et al. Ets1 and Ets2 are required for endothelial cell survival during embryonic angiogenesis. *Blood* (2009).
3. Cases S, et al. Development of the mammary gland requires DGAT1 expression in stromal and epithelial tissues. *Development* 131, 3047-55. (2004).
4. Gunther, E. J. et al. A novel doxycycline-inducible system for the transgenic analysis of mammary gland biology. *FASEB J* 16, 283-92 (2002).
5. Dakappagari, N. K. et al. Conformational HER-2/neu B-cell epitope peptide vaccine designed to incorporate two native disulfide bonds enhances tumor cell binding and antitumor activities. *J Biol Chem* 280, 54-63 (2005).
6. Mook, O. R., Van Overbeek, C., Ackema, E. G., Van Maldegem, F. & Frederiks, W. M. In situ localization of gelatinolytic activity in the extracellular matrix of metastases of colon cancer in rat liver using quenched fluorogenic DQ-gelatin. *J Histochem Cytochem* 51, 821-9 (2003).
7. Irizarry, R. A. et al. Exploration, normalization, and summaries of high density oligonucleotide array probe level data. *Biostatistics* 4, 249-64 (2003).
8. Hu, R. et al. Eos, MITF, and PU.1 recruit corepressors to osteoclast-specific genes in committed myeloid progenitors. *Mol Cell Biol* 27, 4018-27 (2007).

Supplementary Figures:

Supplementary Figure 1: Scheme for the generation of *Pten* conditional mice.

Three *loxP* sites were introduced into two Hpa1 restriction sites (H) within introns 3 and 5 on the *Pten* construct, resulting in the loss of these restriction sites (HΔ). Two of the *loxP* sites were associated with the insertion of a neo cassette, used as the selectable marker. An EcoR V (RV) restriction digest was performed to generate the final construct for delivery into ES cells and integration into the genome via homologous recombination. Limited *-cre* expression resulted in the removal of the neo cassette with the remaining two *loxP* sites flanking *Pten* exon 4 and exon 5. Tissue specific expression of cre removes *Pten* exon 4 and exon 5 from the genome and results in loss of functional Pten expression.

Supplementary Figure 2: Cellular location of *Fsp-cre* expression.

(a) IHC staining for the epithelial markers Cytokeratin 8/18 (Ck8/18) was performed on paraffin sections from X-gal stained mammary tissue (8 week old mice). The Ck 8/18 expression did not overlap with the X-gal marked cre expression generated by *Fsp-cre* and the *Rosa26^{loxP}* reporter.

(b) Macrophage (F4/80) and endothelial cells (CD31) were isolate by flow cytometry, using the indicated cell marker, and epithelial and fibroblasts cells were isolated by cell culture from *Fsp-cre*; *Pten^{f/f}*; *Rosa26^{loxP}* mice. RNA was purified from each cell type and the expression of the conditional *lacZ* reporter gene was quantified by qRT-PCR.

Supplementary: Figure 3: Further characterization of *Fsp-cre* expression.

(a) IHC analysis on non-X-gal stained slides was used to confirm the loss of conditional Pten protein expression due to *Fsp-cre* in mammary gland from 8-9week old mice. Lower panels are higher magnification images of the area enclosed by the rectangle in the upper panels. The dotted red line indicates the epithelial-stroma boundary, lu- Lumen, epi-epithelium and str-stroma.

(b) Double IF was performed to confirm that loss of Pten expression had not occurred in the myoepithelium. Paraffin sections of mammary tissue from 8-9week old mice were used and myoepithelial cells identified by α -smooth muscle actin (Sma) staining; lu- Lumen, epi-epithelium and str-stroma.

Supplementary Figure 4: Fibroblast viability after transplant

Mammary tissue from *Fsp-cre;Rosa26^{loxP}* and *Rosa26^{loxP}* donors were transplanted into wild-type hosts, removed at 16 weeks post-transplantation and assayed for β -galactosidase activity using X-gal staining. This confirmed that fibroblasts would be viable long enough to allow tumors to be formed using the *MMTV-ErbB2* model, which has a 6-7 month latency period.

Supplementary Figure 5: Verification of *Fsp-cre* expression in the 26 week post transplant tumors for the *MMTV-ErbB2* model.

(a) Hematoxylin and eosin (H&E) and X-gal staining of frozen tissue sections shows increased tumor stroma in the *MMTV-ErbB2;Fsp-cre;Pten^{loxP/loxP}* transplants. Tumors from the *MMTV-ErbB2;Pten^{loxP/loxP}* transplants have little to no significant stroma. Unit size is 2mm. Lower β -gal panels are higher magnifications of the corresponding areas outline above by the black squares.

(b) IHC staining for PTEN revealed that the PTEN protein was absent in the stroma (Str) and present in the tumor epithelium (T). The boundary is marked with the dotted red line.

Supplementary Figure 6: Global gene expression analysis in stromal *Pten*-deleted mammary fibroblasts. Total RNA was isolated from primary mammary fibroblasts derived from 8 week-old mice and processed for microarray analysis using Affimetrix chips (see Methods).

(a) Heat-map of upregulated genes in *Pten*-deleted stromal fibroblasts (<4-fold and $p < 10^{-6}$). Genes are listed on the right in descending order magnitude-change.

(b) Heat-map of downregulated genes in *Pten*-deleted stromal fibroblasts (<4-fold and $p < 10^{-6}$). Genes are listed on the right in descending order magnitude-change.

(c) Quantitative RT-PCR analysis of gene expression of representative genes involved in inflammation and wound healing. Gene expression was analyzed in independent experiments and the average between duplicates of a representative sample are shown with standard deviation (d)

Supplementary Figure 7: Collagen expression in the *Pten* deleted mammary gland.

- (a) Masson's Trichrome staining of mammary gland sections with the indicated genotypes at 16 weeks post-transplantation.
- (b) Epithelial cells produce collagen IV as part of the basement membrane, which surround the mammary ducts. To determine if the observed collagen deposits are a result of the expansion of the basement membrane, IF staining was performed using a collagen IV antibody. There was no expansion of the basement membrane as the collagen IV staining (red) was only observed adjacent to the epithelia cells (green; E-cadherin).
- (c). To determine if these ECM deposits were due to an increase in pro-collagen I, protein lysates from primary fibroblasts isolated from 8 week old non-transplanted mammary glands were used for western analysis. An increase in both the pro-collagen and its processed form was observed.

Supplementary Figure 8: F4/80 expression in the *MMTV-ErbB2* model in the presence or absence of *Pten*. Sections from mammary glands transplants with the indicated genotypes were stained with the macrophage-specific marker F4/80.

Supplementary Table 1: *Pten*-responsive genes upregulated more than fourfold in the *Fsp-cre;Pten^{loxP/loxP}* vs. *Pten^{loxP/loxP}* primary mammary stromal cells

Gene Symbol	Gene name	Difference	Reference	Role
<i>Ccl3</i>	chemokine (C-C motif) ligand 3	77.5	1.	inflammation
<i>Irg1</i>	immunoresponsive gene 1	51.6	2.	inflammation
<i>Il1b</i>	interleukin 1 beta	45	3.	inflammation
<i>Ccl12</i>	chemokine (C-C motif) ligand 12	35.5	4.	wound fibrosis
<i>Clec4e</i>	C-type lectin domain family 4, member e	33.2	5.	inflammation
<i>Arg1</i>	arginase 1, liver	20.9	6.	inflammation
<i>Fpr-rs2</i>	formyl peptide receptor, related sequence 2	19.2	7.	inflammation
<i>Fcgr1g</i>	Fc receptor, IgE, high affinity I, gamma polypeptide	18.3	8.	inflammation
<i>Marco</i>	macrophage receptor with collagenous structure	18	9.	inflammation
<i>Ccl6</i>	chemokine (C-C motif) ligand 6	17.2	10.	inflammation
<i>Fpr1</i>	formyl peptide receptor 1	15.9	11.	wound
<i>F13a1</i>	coagulation factor XIII, A1 subunit	15.8	12.	wound
<i>Mmp12</i>	matrix metalloproteinase 12	15.7	13.	wound fibrosis
<i>Lcp1</i>	lymphocyte cytosolic protein 1	14.2	14.	inflammation
<i>Lyzs</i>	lysozyme	14.1	15.	inflammation
<i>S100a3</i>	S100 calcium binding protein A3	13.6	16.	wound ECM
<i>Mpeg1</i> /// <i>LOC671359</i>	macrophage expressed gene 1 /// similar to macrophage expressed gene 1	13.4	17.	inflammation
<i>Msr1</i>	macrophage scavenger receptor 1	13.3	18.	inflammation
<i>Tyrbp</i>	TYRO protein tyrosine kinase binding protein	13.3	19.	Wound ECM
<i>Igfbp5</i>	insulin-like growth factor binding protein 5	13.2	20.	wound fibrosis
<i>Clec4n</i>	C-type lectin domain family 4, member n	13	21.	inflammation
<i>Rac2</i>	RAS-related C3 botulinum substrate 2	12.6	22.	inflammation
<i>Ccl4</i>	chemokine (C-C motif) ligand 4	12	23.	inflammation
<i>Gp49a</i> /// <i>Lilrb4</i>	glycoprotein 49 A /// leukocyte immunoglobulin-like receptor, subfamily B, member 4	11.8	24.	inflammation
<i>Cybb</i>	cytochrome b-245, beta polypeptide	11.6	25.	inflammation
<i>Laptm5</i>	lysosomal-associated protein transmembrane 5	11.4	26.	inflammation
---	CDNA clone MGC:107680 IMAGE:6766535	11.4	N/A	N/A
<i>Plek</i>	pleckstrin	11.3	27.	inflammation
<i>Fcgr2b</i>	Fc receptor, IgG, low affinity IIb	11.1	28.	wound
<i>Clec4d</i>	C-type lectin domain family 4, member d	10.7	29.	inflammation
<i>Cxcl4</i>	chemokine (C-X-C motif) ligand 4	10.6	30.	inflammation
<i>Prg1</i>	proteoglycan 1, secretory granule (Srgn)	10.4	31.	inflammation
<i>Sema4f</i>	sema domain, immunoglobulin domain (Ig), TM domain, and short cytoplasmic domain	10.3	32.	other (neuronal)
<i>Pik3ap1</i>	phosphoinositide-3-kinase adaptor protein 1	10	33.	inflammation
<i>Cd14</i>	CD14 antigen	9.8	34.	inflammation
<i>Cd300lf</i>	CD300 antigen like family member F	9.7	35.	inflammation
<i>Lzp-s</i>	P lysozyme structural	9.3	36.	inflammation
<i>Itgb2</i>	integrin beta 2 (CD18)	9.1	37.	wound healing
<i>Hal</i> /// <i>LOC638196</i>	histidine ammonia lyase /// similar to Histidine ammonia-lyase (Histidase)	8.9	38.	inflammation
<i>Cd48</i>	CD48 antigen	8.6	39.	inflammation
<i>Ptpnc</i>	protein tyrosine phosphatase, receptor type, C (CD45)	8.6	40.	inflammation
---	---	8.5	N/A	N/A

<i>Ctss</i>	cathepsin S	8.5	41.	inflammation
<i>Cd36</i>	CD36 antigen	8.3	42.	inflammation
<i>Ctsc</i>	cathepsin C	8.1	43.	inflammation
<i>Adam8</i>	a disintegrin and metallopeptidase domain 8	8	44.	inflammation
<i>ErbB3</i>	v-erb-b2 erythroblastic leukemia viral oncogene homolog 3 (avian)	8	45.	inflammation
<i>Ms4a6d</i>	membrane-spanning 4-domains, subfamily A, member 6D	7.9	46.	inflammation
<i>Phb</i>	Prohibitin	7.9	47.	inflammation
<i>Hcls1</i>	hematopoietic cell specific Lyn substrate 1	7.8	48.	inflammation
<i>Bcl2a1a</i> /// <i>Bcl2a1b</i> /// <i>Bcl2a1d</i>	B-cell leukemia/lymphoma 2 related protein A1a /// B-cell leukemia/lymphoma 2 related protein A1b /// B-cell leukemia/lymphoma 2 related protein A1d	7.8	49.	inflammation
<i>Ncf1</i>	neutrophil cytosolic factor 1	7.7	50.	inflammation
<i>Rapgef5</i>	Rap guanine nucleotide exchange factor (GEF) 5	7.6	51.	inflammation
<i>Lcp2</i>	lymphocyte cytosolic protein 2	7.6	52.	inflammation
<i>Afp</i>	alpha fetoprotein	7.6	53.	inflammation
<i>Emr1</i>	EGF-like module containing, mucin-like, hormone receptor-like sequence 1	7.4	54.	inflammation
<i>Krt23</i>	keratin 23	7.3	55.	inflammation
<i>Rassf4</i>	Ras association (RalGDS/AF-6) domain family 4	7.3	56.	other
<i>Il2rg</i>	interleukin 2 receptor, gamma chain	7.2	57.	inflammation
<i>C3ar1</i>	complement component 3a receptor 1	7.2	58.	inflammation
<i>2310026E23Rik</i>	RIKEN cDNA 2310026E23 gene	7.1	N/A	N/A
<i>BC032204</i>	cDNA sequence BC032204	7	N/A	N/A
<i>Moxd1</i>	monooxygenase, DBH-like 1	7	59.	inflammation
<i>Pld4</i>	phospholipase D family, member 4	6.9	60.	inflammation
<i>Cd72</i>	CD72 antigen	6.8	61.	inflammation
	glycine amidinotransferase (L-arginine:glycine amidinotransferase)	6.8	62.	inflammation
<i>Gatm</i>		6.8	62.	inflammation
<i>Cd68</i>	CD68 antigen	6.7	63.	inflammation
<i>Fgf5</i>	fibroblast growth factor 5	6.6	64.	wound ECM
<i>Itgb8</i>	integrin beta 8	6.6	65.	wound ECM
<i>Ms4a6b</i>	membrane-spanning 4-domains, subfamily A, member 6B	6.5	66.	inflammation
<i>Tnf</i>	tumor necrosis factor	6.4	67.	inflammation
<i>Cfp</i>	complement factor properdin	6.4	68.	inflammation
	solute carrier family 28 (sodium-coupled nucleoside transporter), member 2 /// similar to solute carrier family 28 (sodium-coupled nucleoside transporter), member 2	6.3	69.	inflammation
<i>Slc28a2</i> /// <i>LOC381417</i>		6.3	69.	inflammation
<i>AI851790</i>	expressed sequence AI851790	6.2	N/A	N/A
<i>Igsf4a</i>	immunoglobulin superfamily, member 4A (Cadm1)	6.2	70.	other (tumor suppressor)
<i>Cxcl2</i>	chemokine (C-X-C motif) ligand 2	6.2	71.	inflammation
<i>Igsf6</i>	immunoglobulin superfamily, member 6	6	72.	inflammation
<i>Osm</i>	oncostatin M	6	73.	Wound
---	Transcribed locus	6	N/A	N/A
<i>1100001H23Rik</i>	RIKEN cDNA 1100001H23 gene	5.8	N/A	N/A
<i>Hdgfrp3</i> /// <i>Tm6sf1</i>	hepatoma-derived growth factor, related protein 3 /// transmembrane 6 superfamily member 1	5.8	74.	inflammation
<i>Hemt1</i>	hematopoietic cell transcript 1	5.7	75.	other
<i>Csf2rb2</i>	colony stimulating factor 2 receptor, beta 2, low-affinity (granulocyte-macrophage)	5.7	76.	inflammation
<i>Hk3</i>	hexokinase 3	5.6	77.	other

				metabolism
<i>Lpxn</i>	leupaxin	5.6	78.	inflammation
<i>Fcgr3</i>	Fc receptor, IgG, low affinity III	5.6	79.	inflammation
<i>Was</i>	Wiskott-Aldrich syndrome homolog (human)	5.5	80.	inflammation
<i>Selpl</i>	selectin, platelet (p-selectin) ligand	5.5	81.	inflammation
<i>C5ar1</i>	complement component 5a receptor 1	5.3	82.	inflammation
<i>L1cam</i>	L1 cell adhesion molecule	5.3	83.	wound ECM
<i>Igsf4c</i>	immunoglobulin superfamily, member 4C	5.3	84.	other adhesion
<i>Ncf4</i>	neutrophil cytosolic factor 4	5.1	85.	inflammation
<i>Pilrb1</i>	paired immunoglobulin-like type 2 receptor beta 1	5.1	86.	other
<i>Ly9</i>	lymphocyte antigen 9	5.1	87.	inflammation
<i>Krt19</i>	keratin 19	5	88.	inflammation
<i>Ikzf1</i>	IKAROS family zinc finger 1	5	89.	inflammation
<i>Nckap1l</i>	NCK associated protein 1 like (Hem 1)	5	90.	inflammation
<i>Clec4a2</i>	C-type lectin domain family 4, member a2	5	91.	inflammation
<i>LOC668101</i>	similar to SIRP beta 1 isoform 2	4.9	N/A	N/A
<i>Ptpn6</i>	protein tyrosine phosphatase, non-receptor type 6	4.8	92.	inflammation
<i>BC013712</i>	cDNA sequence BC013712	4.8	93.	inflammation
<i>Ccr1</i>	chemokine (C-C motif) receptor 1	4.8	94.	inflammation
<i>AI662270</i>	expressed sequence AI662270	4.8	N/A	N/A
<i>Npy</i>	neuropeptide Y	4.7	95.	inflammation
<i>Irf8</i>	interferon regulatory factor 8	4.7	96.	inflammation
<i>Slc13a3</i>	solute carrier family 13 (sodium-dependent dicarboxylate transporter), member 3	4.7	97.	other Krebs cycle
<i>Ms4a6c</i>	membrane-spanning 4-domains, subfamily A, member 6C	4.7	N/A	N/A
<i>Tlr13</i>	toll-like receptor 13	4.6	98.	inflammation
<i>Dock10 /// LOC630691</i>	dedicator of cytokinesis 10 /// similar to Dedicator of cytokinesis protein 10 (Protein zizimin 3)	4.6	99.	wound ECM
<i>Apold1</i>	apolipoprotein L domain containing 1	4.5	100.	other (neuro)
<i>Mrc1</i>	mannose receptor, C type 1	4.5	101.	inflammation
<i>Ms4a7</i>	membrane-spanning 4-domains, subfamily A, member 7	4.5	102.	inflammation
<i>Edil3</i>	EGF-like repeats and discoidin I-like domains 3	4.4	103.	wound ECM
<i>Pla2g7</i>	phospholipase A2, group VII (platelet-activating factor acetylhydrolase, plasma)	4.4	104.	inflammation
<i>Kctd12</i>	potassium channel tetramerisation domain containing 12	4.4	105.	other markers
<i>Tlr7</i>	toll-like receptor 7	4.3	106.	inflammation
<i>Gpr109a</i>	G protein-coupled receptor 109A	4.3	107.	inflammation
<i>Vav3</i>	vav 3 oncogene	4.3	108.	Wound ECM
<i>Cd53</i>	CD53 antigen	4.3	109.	inflammation
<i>Plp1</i>	proteolipid protein (myelin) 1	4.3	110.	inflammation
<i>Lonrf3</i>	LON peptidase N-terminal domain and ring finger 3	4.2	N/A	N/A
<i>Lgi1</i>	leucine-rich repeat LGI family, member 1	4.2	111.	other neuro
<i>Gm1960 /// Cxcl3</i>	gene model 1960, (NCBI)	4.2	112.	inflammation
<i>Cd52</i>	CD52 antigen	4.2	113.	inflammation
<i>Sh3bgrl2</i>	SH3 domain binding glutamic acid-rich protein like 2	4.1	114.	other heart devel
<i>Rnf128</i>	ring finger protein 128 (Grail)	4.1	115.	inflammation
<i>Ncf2</i>	neutrophil cytosolic factor 2	4.1	116.	inflammation
<i>Cd93</i>	CD93 antigen	4.1	117.	inflammation
<i>Cd84</i>	CD84 antigen	4.1	118.	inflammation

<i>Rasgef1b</i>	RasGEF domain family, member 1B	4	119.	other develop
<i>Ebi3</i>	Epstein-Barr virus induced gene 3	4	120.	inflammation
<i>Pdgfb</i>	platelet derived growth factor, B polypeptide	4	121.	wound fibrosis

Biological roles affected by the genes upregulated in *Fsp-Cre;Pten^{loxP/loxP}*

1. [DiPietro LA, Burdick M, Low QE, Kunkel SL, Strieter RM.](#) (1998). MIP-1alpha as a critical macrophage chemoattractant in murine wound repair. *J Clin Invest.* 101, 1693-1698.
2. [Lund S, Christensen KV, Hedtjarn M, Mortensen AL, Hagberg H, Falsig J, Hasseldam H, Schrattenholz A, Porzgen P, Leist M.](#) (2006). The dynamics of the LPS triggered inflammatory response of murine microglia under different culture and in vivo conditions. *J Neuroimmunol.* 180, 71-87.
3. [Church LD, Cook GP, McDermott MF.](#) (2008). Primer: inflammasomes and interleukin 1beta in inflammatory disorders. *Nat Clin Pract Rheumatol.* 2008 Jan;4(1):34-42.
4. [Moore BB, Murray L, Das A, Wilke CA, Herrrygers AB, Toews GB.](#) (2006). The role of CCL12 in the recruitment of fibrocytes and lung fibrosis. *Am. J. Respir. Cell. Mol. Biol.* 35,175-181.
5. [Nakamura N, Shimaoka Y, Tougan T, Onda H, Okuzaki D, Zhao H, Fujimori A, Yabuta N, Nagamori I, Tanigawa A, Sato J, Oda T, Hayashida K, Suzuki R, Yukioka M, Nojima H, Ochi T.](#) (2006). Isolation and expression profiling of genes upregulated in bone marrow-derived mononuclear cells of rheumatoid arthritis patients. *DNA Res.* 13, 169-183.
6. [Viola A, Bronte V.](#) (2007). Metabolic mechanisms of cancer-induced inhibition of immune responses. *Semin Cancer Biol.* 17, 309-316.
7. [Migeotte I, Communi D, Parmentier M.](#) (2006). Formyl peptide receptors: a promiscuous subfamily of G protein-coupled receptors controlling immune responses. *Cytokine Growth Factor Rev.* 17, 501-519.
8. [Gould HJ, Sutton BJ.](#) (2008). IgE in allergy and asthma today. *Nat. Rev. Immunol.* 8, 205-217.
9. [Granucci F, Petralia F, Urbano M, Citterio S, Di Tota F, Santambrogio L, Ricciardi-Castagnoli P.](#) (2003). The scavenger receptor MARCO mediates cytoskeleton rearrangements in dendritic cells and microglia. *Blood* 102, 2940-2947
10. [Coelho AL, Schaller MA, Benjamim CF, Orlofsky AZ, Hogaboam CM, Kunkel SL.](#) (2007). The chemokine CCL6 promotes innate immunity via immune cell activation and recruitment. *J. Immunol.* 179, 5474-5482.
11. [Babbitt BA, Jesaitis AJ, Ivanov AI, Kelly D, Laukoetter M, Nava P, Parkos CA, Nusrat A.](#) (2007). Formyl peptide receptor-1 activation enhances intestinal epithelial cell restitution through phosphatidylinositol 3-kinase-dependent activation of Rac1 and Cdc42. *J. Immunol.* 179, 8112-8121.
12. [Tognazzo S, Gemmati D, Palazzo A, Catozzi L, Carandina S, Legnaro A, Tacconi G, Scapoli GL, Zamboni P.](#) (2006). Prognostic role of factor XIII gene variants in nonhealing venous leg ulcers. *J Vasc Surg.* 44, 815-819.
13. [Matute-Bello G, Wurfel MM, Lee JS, Park DR, Frevert CW, Madtes DK, Shapiro SD, Martin TR.](#) (2007). Essential role of MMP-12 in Fas-induced lung fibrosis. *Am J Respir Cell Mol Biol.* 37, 210-221.
14. [Janji B, Giganti A, De Corte V, Catillon M, Bruyneel E, Lentz D, Plastino J, Gettemans J, Friederich E.](#) (2006). Phosphorylation on Ser5 increases the F-actin-binding activity of L-plastin and promotes its targeting to sites of actin assembly in cells. *J Cell Sci.* 2006 May 1;119(Pt 9):1947-60.
15. [Lei W, Jaramillo RJ, Harrod KS.](#) (2007). Transactivation of lung lysozyme expression by Ets family member ESE-1. *Am J Physiol Lung Cell Mol Physiol.* 293, L1359-1368.
16. [Eckert RL, Broome AM, Ruse M, Robinson N, Ryan D, Lee K.](#) S100 proteins in the epidermis. (2004). *J Invest Dermatol.* 123, 23-33.
17. [Sester DP, Trieu A, Brion K, Schroder K, Ravasi T, Robinson JA, McDonald RC, Ripoll V, Wells CA, Suzuki H, Hayashizaki Y, Stacey KJ, Hume DA, Sweet MJ.](#) (2005). LPS regulates a set of genes in primary murine macrophages by antagonising CSF-1 action. *Immunobiology* 210, 97-107.
18. [Sun J, Turner A, Xu J, Grönberg H, Isaacs W.](#) (2007). Genetic variability in inflammation pathways and prostate cancer risk. *Urol Oncol.* 25, 250-259.
19. [Turnbull IR, Colonna M.](#) (2007). Activating and inhibitory functions of DAP12. *Nat Rev Immunol.* 7, 155-161.

20. [Yasuoka H, Zhou Z, Pilewski JM, Oury TD, Choi AM, Feghali-Bostwick CA.](#) (2006). Insulin-like growth factor-binding protein-5 induces pulmonary fibrosis and triggers mononuclear cellular infiltration. *Am J Pathol.* 169, 1633-1642.
21. [Gavino AC, Chung JS, Sato K, Ariizumi K, Cruz PD Jr.](#) (2005). Identification and expression profiling of a human C-type lectin, structurally homologous to mouse dectin-2. *Exp Dermatol.* 14, 281-288.
22. [Arana E, Vehlow A, Harwood NE, Vigorito E, Henderson R, Turner M, Tybulewicz VL, Batista FD.](#) (2008). Activation of the small GTPase Rac2 via the B cell receptor regulates B cell adhesion and immunological-synapse formation. *Immunity* 28, 88-99.
23. [Zhang T, Guo CJ, Li Y, Douglas SD, Qi XX, Song L, Ho WZ.](#) (2003). Interleukin-1beta induces macrophage inflammatory protein-1beta expression in human hepatocytes. *Cell Immunol.* 226, 45-53
24. [Katz HR.](#) (2007). Inhibition of pathologic inflammation by leukocyte Ig-like receptor B4 and related inhibitory receptors. *Immunol Rev.* 217, 222-230.
25. [Savina A, Jancic C, Hugues S, Guermonprez P, Vargas P, Moura IC, Lennon-Dumenil AM, Seabra MC, Raposo G, Amigorena S.](#) (2006). NOX2 controls phagosomal pH to regulate antigen processing during crosspresentation by dendritic cells. *Cell* 126, 205-218.
26. [Seimiya M, O-Wang J, Bahar R, Kawamura K, Wang Y, Saisho H, Tagawa M.](#) (2003). Stage-specific expression of Clast6/E3/LAPTM5 during B cell differentiation: elevated expression in human B lymphomas. *Int J Oncol.* 22, 301-304.
27. [Hawkins PT, Stephens LR.](#) (2007). PI3Kgamma is a key regulator of inflammatory responses and cardiovascular homeostasis. *Science* 318, 64-66.
28. [Nakamura A, Yuasa T, Ujike A, Ono M, Nukiwa T, Ravetch JV, Takai T.](#) (1999). Fcgamma receptor IIB-deficient mice develop Goodpasture's syndrome upon immunization with type IV collagen: a novel murine model for autoimmune glomerular basement membrane disease. *J Exp Med.* 189, 1573-1579.
29. [Arce I, Martinez-Munoz L, Roda-Navarro P, Fernandez-Ruiz E.](#) (2004). The human C-type lectin CLECSF8 is a novel monocyte/macrophage endocytic receptor. *Eur J Immunol.* 34, 210-220.
30. [Cervi D, Yip TT, Bhattacharya N, Podust VN, Peterson J, Abou-Slaybi A, Naumov GN, Bender E, Almog N, Italiano JE Jr, Folkman J, Klement GL.](#) (2008). Platelet-associated PF-4 as a biomarker of early tumor growth. *Blood*, 111: 1201-1207.
31. [Robinson L, Panayiotakis A, Papas TS, Kola I, Seth A.](#) (1997). ETS target genes: identification of *egr1* as a target by RNA differential display and whole genome PCR techniques. *Proc Natl Acad Sci U S A.* 94, 7170-7175.
32. [Schultze W, Eulenburg V, Lessmann V, Herrmann L, Dittmar T, Gundelfinger ED, Heumann R, Erdmann KS.](#) (2001). Semaphorin4F interacts with the synapse-associated protein SAP90/PSD-95. *J Neurochem.* 78, 482-489.
33. [Yamazaki T, Kurosaki T.](#) (2003). Contribution of BCAP to maintenance of mature B cells through c-Rel. *Nat Immunol.* 4, 780-786.
34. [Zhao Z, Fleming R, McCloud B, Klempner MS.](#) (2007). CD14 mediates cross talk between mononuclear cells and fibroblasts for upregulation of matrix metalloproteinase 9 by *Borrelia burgdorferi*. *Infect Immun.* 75, 3062-3069.
35. [Alvarez-Errico D, Sayos J, Lopez-Botet M.](#) (2007). The IREM-1 (CD300f) inhibitory receptor associates with the p85alpha subunit of phosphoinositide 3-kinase. *J Immunol.* 178, 808-816.
36. [Tanabe H, Ayabe T, Bainbridge B, Guina T, Ernst RK, Darveau RP, Miller SI, Ouellette AJ.](#) (2005). Mouse paneth cell secretory responses to cell surface glycolipids of virulent and attenuated pathogenic bacteria. *Infect Immun.* 73, 2312-2320.
37. [Peters T, Sindrilaru A, Hinz B, Hinrichs R, Menke A, Al-Azzeh EA, Holzwarth K, Oreshkova T, Wang H, Kess D, Walzog B, Sulyok S, Sunderkotter C, Friedrich W, Wlaschek M, Krieg T, Scharffetter-Kochanek K.](#) (2005). Wound-healing defect of CD18(-/-) mice due to a decrease in TGF-beta1 and myofibroblast differentiation. *EMBO J.* 24, 3400-3410.
38. [Pilbak S, Tomin A, Retey J, Poppe L.](#) (2006). The essential tyrosine-containing loop conformation and the role of the C-terminal multi-helix region in eukaryotic phenylalanine ammonia-lyases. *FEBS J.* 273, 1004-1019.
39. [Gonzalez-Cabrero J, Wise CJ, Latchman Y, Freeman GJ, Sharpe AH, Reiser H.](#) (1999). CD48-deficient mice have a pronounced defect in CD4(+) T cell activation. *Proc Natl Acad Sci U S A.* 1999 Feb 2;96(3):1019-23.

40. [van Vliet SJ, Gringhuis SI, Geijtenbeek TB, van Kooyk Y. \(2006\).](#) Regulation of effector T cells by antigen-presenting cells via interaction of the C-type lectin MGL with CD45. *Nat Immunol.* 7, 1200-1208.
41. [Wiendl H, Lautwein A, Mitsdorffer M, Krause S, Erfurth S, Wienhold W, Morgalla M, Weber E, Overkleef HS, Lochmuller H, Melms A, Tolosa E, Driessen C. \(2003\).](#) Antigen processing and presentation in human muscle: cathepsin S is critical for MHC class II expression and upregulated in inflammatory myopathies. *J Neuroimmunol.* 138, 132-43.
42. [Moodley Y, Rigby P, Bundell C, Bunt S, Hayashi H, Misso N, McNulty R, Laurent G, Scaffidi A, Thompson P, Knight D. \(2003\).](#) Macrophage recognition and phagocytosis of apoptotic fibroblasts is critically dependent on fibroblast-derived thrombospondin 1 and CD36. *Am J Pathol.* 162, 771-779.
43. [Appleton CT, Pitelka V, Henry J, Beier F. \(2007\).](#) Global analyses of gene expression in early experimental osteoarthritis. *Arthritis Rheum.* 56, 1854-1868.
44. [Foley SC, Mogas AK, Olivenstein R, Fiset PO, Chakir J, Bourbeau J, Ernst P, Lemièrre C, Martin JG, Hamid Q. \(2007\).](#) Increased expression of ADAM33 and ADAM8 with disease progression in asthma. *J Allergy Clin Immunol.* 119, 863-871.
45. [Vijapurkar U, Kim MS, Koland JG. \(2003\).](#) Roles of mitogen-activated protein kinase and phosphoinositide 3'-kinase in ErbB2/ErbB3 coreceptor-mediated heregulin signaling. *Exp Cell Res.* 284, 291-302.
46. [Kim U, Siegel R, Ren X, Gunther CS, Gaasterland T, Roeder RG. \(2003\).](#) Identification of transcription coactivator OCA-B-dependent genes involved in antigen-dependent B cell differentiation by cDNA array analyses. *Proc Natl Acad Sci U S A.* 100, 8868-8873.
47. [Mishra S, Murphy LC, Nyomba BL, Murphy LJ. \(2005\).](#) Prohibitin: a potential target for new therapeutics. *Trends Mol Med.* 11, 192-197.
48. [Fischer U, Michel A, Meese EU. \(2005\).](#) Expression of the gene for hematopoietic cell specific protein is not restricted to cells of hematopoietic origin. *Int J Mol Med.* 15, 611-615.
49. [He CH, Waxman AB, Lee CG, Link H, Rabach ME, Ma B, Chen Q, Zhu Z, Zhong M, Nakayama K, Nakayama KI, Homer R, Elias JA. \(2005\).](#) Bcl-2-related protein A1 is an endogenous and cytokine-stimulated mediator of cytoprotection in hyperoxic acute lung injury. *J Clin Invest.* 115, 1039-1048.
50. [Hultqvist M, Holmdahl R. \(2005\).](#) Ncf1 (p47phox) polymorphism determines oxidative burst and the severity of arthritis in rats and mice. *Cell Immunol.* 233, 97-101.
51. [Hong J, Doebele RC, Linggen MW, Quilliam LA, Tang WJ, Rosner MR. \(2007\).](#) Anthrax edema toxin inhibits endothelial cell chemotaxis via Epac and Rap1. *J Biol Chem.* 282, 19781-19787.
52. [Koretzky GA, Abtahian F, Silverman MA. \(2006\).](#) SLP76 and SLP65: complex regulation of signalling in lymphocytes and beyond. *Nat Rev Immunol.* 6, 67-78.
53. [Mizukoshi E, Nakamoto Y, Tsuji H, Yamashita T, Kaneko S. \(2006\).](#) Identification of alpha-fetoprotein-derived peptides recognized by cytotoxic T lymphocytes in HLA-A24+ patients with hepatocellular carcinoma. *Int J Cancer* 118, 1194-1204.
54. [Hamann J, Koning N, Pouwels W, Ulfman LH, van Eijk M, Stacey M, Lin HH, Gordon S, Kwakkenbos MJ. \(2007\).](#) EMR1, the human homolog of F4/80, is an eosinophil-specific receptor. *Eur J Immunol.* 37, 2797-2802.
55. [Suzuki A, Ji G, Numabe Y, Muramatsu M, Gomi K, Kanazashi M, Ogata Y, Shimizu E, Shibukawa Y, Ito A, Ito T, Sugaya A, Arai T, Yamada S, Deguchi S, Kamo K. \(2004\).](#) Single nucleotide polymorphisms associated with aggressive periodontitis and severe chronic periodontitis in Japanese. *Biochem Biophys Res Commun.* 317, 887-892.
56. [Eckfeld K, Hesson L, Vos MD, Bieche I, Latif F, Clark GJ. \(2004\).](#) RASSF4/AD037 is a potential ras effector/tumor suppressor of the RASSF family. *Cancer Res.* 64, 8688-8693.
57. [Doucet C, Giron-Michel J, Canonica GW, Azzarone B. \(2002\).](#) Human lung myofibroblasts as effectors of the inflammatory process: the common receptor gamma chain is induced by Th2 cytokines, and CD40 ligand is induced by lipopolysaccharide, thrombin and TNF-alpha. *Eur J Immunol.* 32, 2437-2449.
58. [Hasegawa K, Tamari M, Shao C, Shimizu M, Takahashi N, Mao XQ, Yamasaki A, Kamada F, Doi S, Fujiwara H, Miyatake A, Fujita K, Tamura G, Matsubara Y, Shirakawa T, Suzuki Y. \(2004\).](#) Variations in the C3, C3a receptor, and C5 genes affect susceptibility to bronchial asthma. *Hum Genet.* 115, 295-301.
59. [Xin X, Mains RE, Eipper BA. \(2004\).](#) Monooxygenase X, a member of the copper-dependent monooxygenase family localized to the endoplasmic reticulum. *J Biol Chem.* 279, 48159-48167.

60. [Powner DJ, Hodgkin MN, Wakelam MJ. \(2002\).](#) Antigen-stimulated activation of phospholipase D1b by Rac1, ARF6, and PKCalpha in RBL-2H3 cells. *Mol Biol Cell.* 13, 1252-1262.
61. [Aoshiba K, Nagai A. \(2007\).](#) Chronic lung inflammation in aging mice. *FEBS Lett.* 581, 3512-3516.
62. [Sandell LL, Guan XJ, Ingram R, Tilghman SM. \(2003\).](#) Gattm, a creatine synthesis enzyme, is imprinted in mouse placenta. *Proc Natl Acad Sci U S A.* 100, 4622-4627.
63. [Kunz-Schughart LA, Weber A, Rehli M, Gottfried E, Brockhoff G, Krause SW, Andreesen R, Kreutz M. \(2003\).](#) [The "classical" macrophage marker CD68 is strongly expressed in primary human fibroblasts] *Verh Dtsch Ges Pathol.* 87, 215-223.
64. [Sieuwerts AM, Martens JW, Dorssers LC, Klijn JG, Foekens JA. \(2002\).](#) Differential effects of fibroblast growth factors on expression of genes of the plasminogen activator and insulin-like growth factor systems by human breast fibroblasts. *Thromb Haemost.* 87, 674-683
65. [Pae SH, Dokic D, Dettman RW. \(2008\).](#) Communication between integrin receptors facilitates epicardial cell adhesion and matrix organization. *Dev Dyn.* 237, 962-978
66. [Adarichev VA, Vermes C, Hanyecz A, Mikecz K, Bremer EG, Glant TT. \(2005\).](#) Gene expression profiling in murine autoimmune arthritis during the initiation and progression of joint inflammation. *Arthritis Res Ther.* 7, R196-207.
67. [Balkwill F. \(2006\).](#) TNF-alpha in promotion and progression of cancer. *Cancer Metastasis Rev.* 25, 409-416.
68. [Kimura Y, Miwa T, Zhou L, Song WC. \(2008\).](#) Activator-specific requirement of properdin in the initiation and amplification of the alternative pathway complement. *Blood* 111, 732-740.
69. [Fernández-Veledo S, Jover R, Casado FJ, Gómez-Lechón MJ, Pastor-Anglada M. \(2007\).](#) Transcription factors involved in the expression of SLC28 genes in human liver parenchymal cells. *Biochem Biophys Res Commun.* 353, 381-388.
70. [Heller G, Fong KM, Girard L, Seidl S, End-Pfützenreuter A, Lang G, Gazdar AF, Minna JD, Zielinski CC, Zöchbauer-Müller S. \(2006\).](#) Expression and methylation pattern of TSLC1 cascade genes in lung carcinomas. *Oncogene* 25, 959-968.
71. [Zhang XW, Liu Q, Wang Y, Thorlacius H. \(2001\).](#) CXC chemokines, MIP-2 and KC, induce P-selectin-dependent neutrophil rolling and extravascular migration in vivo. *Br J Pharmacol.* 133, 413-421.
72. [Bates EE, Kissenpfennig A, Peronne C, Mattei MG, Fossiez F, Malissen B, Lebecque S. \(2003\).](#) Genetic variation in the IGSF6 gene and lack of association with inflammatory bowel disease. *Eur J Immunogenet.* 30, 187-190.
73. [Fearon U, Mullan R, Markham T, Connolly M, Sullivan S, Poole AR, FitzGerald O, Bresnihan B, Veale DJ. \(2006\).](#) Oncostatin M induces angiogenesis and cartilage degradation in rheumatoid arthritis synovial tissue and human cartilage cocultures. *Arthritis Rheum.* 54, 3152-3162.
74. [Abouzie MM, Baader SL, Dietz F, Kappler J, Gieselmann V, Franken S. \(2004\).](#) Expression patterns and different subcellular localization of the growth factors HDGF (hepatoma-derived growth factor) and HRP-3 (HDGF-related protein-3) suggest functions in addition to their mitogenic activity. *Biochem J.* 378, 169-176.
75. [Xue H, O'Neill D, Morrow J, Bank A. \(1999\).](#) A novel mouse gene, HemT, encoding an hematopoietic cell-specific transcript. *Gene* 231, 49-58.
76. [Paling NR, Welham MJ. \(2002\).](#) Role of the protein tyrosine phosphatase SHP-1 (Src homology phosphatase-1) in the regulation of interleukin-3-induced survival, proliferation and signalling. *Biochem J.* 368, 885-894.
77. [Hoofst L, van der Veldt AA, Hoekstra OS, Boers M, Molthoff CF, van Diest PJ. \(2008\).](#) Hexokinase III, cyclin A and galectin-3 are overexpressed in malignant follicular thyroid nodules. *Clin Endocrinol (Oxf)* 2, 252-257.
78. [Watanabe N, Amano N, Ishizuka H, Mashima K. \(2005\).](#) Leupaxin binds to PEST domain tyrosine phosphatase PEP. *Mol Cell Biochem.* 269, 13-17.
79. [Díaz de Ståhl T, Andrén M, Martinsson P, Verbeek JS, Kleinau S. \(2002\).](#) Expression of FcγRIII is required for development of collagen-induced arthritis. *Eur J Immunol* 32, 2915-2922.
80. [Curcio C, Pannellini T, Lanzardo S, Forni G, Musiani P, Antón IM. \(2007\).](#) WIP null mice display a progressive immunological disorder that resembles Wiskott-Aldrich syndrome. *J. Pathol.* 211, 67-75.
81. [Ley K, Kansas GS. \(2004\).](#) Selectins in T-cell recruitment to non-lymphoid tissues and sites of inflammation. *Nat Rev Immunol* 4, 325-335.

82. [Wrann CD, Winter SW, Barkhausen T, Hildebrand F, Krettek C, Riedemann NC. \(2007\).](#) Distinct involvement of p38-, ERK1/2 and PKC signaling pathways in C5a-mediated priming of oxidative burst in phagocytic cells. *Cell Immunol.* 245, 63-69.
83. [Gast D, Riedle S, Issa Y, Pfeifer M, Beckhove P, Sanderson MP, Arlt M, Moldenhauer G, Fogel M, Krüger A, Altevogt P. \(2008\).](#) The cytoplasmic part of L1-CAM controls growth and gene expression in human tumors that is reversed by therapeutic antibodies. *Oncogene* 27, 1281-1289.
84. [Williams YN, Masuda M, Sakurai-Yageta M, Maruyama T, Shibuya M, Murakami Y. \(2006\).](#) Cell adhesion and prostate tumor-suppressor activity of TSLL2/IGSF4C, an immunoglobulin superfamily molecule homologous to TSLC1/IGSF4. *Oncogene* 25, 1446-1453.
85. [Rioux JD, Xavier RJ, Taylor KD, Silverberg MS, Goyette P, Huett A, Green T, Kuballa P, Barmada MM, Datta LW, Shugart YY, Griffiths AM, Targan SR, Ippoliti AF, Bernard EJ, Mei L, Nicolae DL, Regueiro M, Schumm LP, Steinhardt AH, Rotter JJ, Duerr RH, Cho JH, Daly MJ, Brant SR. \(2007\).](#) Genome-wide association study identifies new susceptibility loci for Crohn disease and implicates autophagy in disease pathogenesis. *Nat Genet.* 39, 596-604
86. [Wilson MD, Cheung J, Martindale DW, Scherer SW, Koop BF. \(2006\).](#) Comparative analysis of the paired immunoglobulin-like receptor (PILR) locus in six mammalian genomes: duplication, conversion, and the birth of new genes. *Physiol Genomics* 27, 201-218.
87. [Graham DB, Bell MP, McCausland MM, Huntoon CJ, van Deursen J, Faubion WA, Crotty S, McKean DJ. \(2006\).](#) Ly9 (CD229)-deficient mice exhibit T cell defects yet do not share several phenotypic characteristics associated with SLAM- and SAP-deficient mice. *J Immunol.* 176, 291-300.
88. [Tao GZ, Strnad P, Zhou Q, Kamal A, Zhang L, Madani ND, Kugathasan S, Brant SR, Cho JH, Omary MB, Duerr RH. \(2007\).](#) Analysis of keratin polypeptides 8 and 19 variants in inflammatory bowel disease. *Clin Gastroenterol Hepatol.* 5, 857-864.
89. [Ezzat S, Mader R, Yu S, Ning T, Poussier P, Asa SL. \(2005\).](#) Ikaros integrates endocrine and immune system development. *J Clin Invest.* 115, 1021-1029.
90. [Weiner OD, Rentel MC, Ott A, Brown GE, Jedrychowski M, Yaffe MB, Gygi SP, Cantley LC, Bourne HR, Kirschner MW. \(2006\).](#) Hem-1 complexes are essential for Rac activation, actin polymerization, and myosin regulation during neutrophil chemotaxis. *PLoS Biol.* 4, e38.
91. [Richard M, Veilleux P, Rouleau M, Paquin R, Beaulieu AD. \(2002\).](#) The expression pattern of the ITIM-bearing lectin CLECSF6 in neutrophils suggests a key role in the control of inflammation. *J Leukoc Biol.* 71, 871-880.
92. [Ostman A, Hellberg C, Bohmer FD. \(2006\).](#) Protein-tyrosine phosphatases and cancer. *Nat Rev Cancer* 6, 307-320.
93. [Treeck O, Kindzorra I, Pauser K, Treeck L, Ortmann O. \(2005\).](#) Expression of icb-1 gene is interferon-gamma inducible in breast and ovarian cancer cell lines and affects the IFN gamma-response of SK-OV-3 ovarian cancer cells. *Cytokine* 32, 137-142.
94. [Vielhauer V, Berning E, Eis V, Kretzler M, Segerer S, Strutz F, Horuk R, Grone HJ, Schlondorff D, Anders HJ. \(2004\).](#) CCR1 blockade reduces interstitial inflammation and fibrosis in mice with glomerulosclerosis and nephrotic syndrome. *Kidney Int.* 66, 2264-2278.
95. [Prod'homme T, Weber MS, Steinman L, Zamvil SS. \(2006\).](#) A neuropeptide in immune-mediated inflammation, Y? *Trends Immunol.* 27, 164-167.
96. [Unlu S, Kumar A, Waterman WR, Tsukada J, Wang KZ, Galson DL, Auron PE. \(2007\).](#) Phosphorylation of IRF8 in a pre-associated complex with Spi-1/PU.1 and non-phosphorylated Stat1 is critical for LPS induction of the IL1B gene. *Mol Immunol.* 44, 3364-79.
97. [Bai XY, Chen X, Sun AQ, Feng Z, Hou K, Fu B. \(2007\).](#) Membrane topology structure of human high-affinity, sodium-dependent dicarboxylate transporter. *FASEB J.* 21, 2409-2417.
98. [West AP, Koblansky AA, Ghosh S. \(2006\).](#) Recognition and signaling by toll-like receptors. *Annu Rev Cell Dev Biol.* 22: 409-437.
99. [Fluge O, Bruland O, Akslen LA, Lillehaug JR, Varhaug JE. \(2006\).](#) Gene expression in poorly differentiated papillary thyroid carcinomas. *Thyroid* 16, 161-175.
100. [Regard JB, Cheek S, Borbiev T, Lanahan AA, Schneider A, Demetriades AM, Hiemisch H, Barnes CA, Verin AD, Worley PF. \(2004\).](#) Verge: a novel vascular early response gene. *J Neurosci* 24, 4092-4103.
101. [Li X, Fleis RI, Shubitowski DM, Ramadas RA, Ewart SL. \(2007\).](#) Fine mapping of murine asthma quantitative trait loci and analyses of Ptg1 and Mrc1 as positional candidate genes. *DNA Seq.* 18, 190-195.

102. [Gingras MC, Lapillonne H, Margolin JF.](#) (2001). CFFM4: a new member of the CD20/FcepsilonRIbeta family. *Immunogenetics* 53, 468-476.
103. [Hidai C, Kawana M, Kitano H, Kokubun S.](#) (2007). Discoidin domain of Del1 protein contributes to its deposition in the extracellular matrix. *Cell Tissue Res.* 330, 83-95.
104. [Nair S, Lee YH, Rousseau E, Cam M, Tataranni PA, Baier LJ, Bogardus C, Permana PA.](#) (2005). Increased expression of inflammation-related genes in cultured preadipocytes/stromal vascular cells from obese compared with non-obese Pima Indians. *Diabetologia* 48, 1784-1788.
105. [Igarashi A, Segoshi K, Sakai Y, Pan H, Kanawa M, Higashi Y, Sugiyama M, Nakamura K, Kurihara H, Yamaguchi S, Tsuji K, Kawamoto T, Kato Y.](#) (2007). Selection of Common Markers for Bone Marrow Stromal Cells from Various Bones Using Real-Time RT-PCR: Effects of Passage Number and Donor Age. *Tissue Eng.* 13, 2405-2417.
106. [Chen CJ, Kono H, Golenbock D, Reed G, Akira S, Rock KL.](#) (2007). Identification of a key pathway required for the sterile inflammatory response triggered by dying cells. *Nat Med.* 13, 851-856.
107. [Offermanns S.](#) (2006). The nicotinic acid receptor GPR109A (HM74A or PUMA-G) as a new therapeutic target. *Trends Pharmacol Sci.* 27, 384-390.
108. [Pearce AC, McCarty OJ, Calaminus SD, Vigorito E, Turner M, Watson SP.](#) (2007). Vav family proteins are required for optimal regulation of PLCgamma2 by integrin alphaIIb beta3. *Biochem J.* 401, 753-761.
109. [Yunta M, Lazo PA.](#) (2003). Apoptosis protection and survival signal by the CD53 tetraspanin antigen. *Oncogene.* 22, 1219-1224.
110. [Karim SA, Barrie JA, McCulloch MC, Montague P, Edgar JM, Kirkham D, Anderson TJ, Nave KA, Griffiths IR, McLaughlin M.](#) (2007). PLP overexpression perturbs myelin protein composition and myelination in a mouse model of Pelizaeus-Merzbacher disease. *Glia* 55, 341-351.
111. [Fukata Y, Adesnik H, Iwanaga T, Bredt DS, Nicoll RA, Fukata M.](#) (2006). Epilepsy-related ligand/receptor complex LGI1 and ADAM22 regulate synaptic transmission. *Science* 313, 1792-1795.
112. [Verhaeghe C, Remouchamps C, Hennuy B, Vanderplasschen A, Chariot A, Tabruyn SP, Oury C, Bours V.](#) (2007). Role of IKK and ERK pathways in intrinsic inflammation of cystic fibrosis airways. *Biochem Pharmacol.* 73, 1982-1994.
113. [Weaver TA, Kirk AD.](#) (2007). Alemtuzumab. *Transplantation* 84, 1545-1547.
114. [Mazzocco M, Maffei M, Egeo A, Vergano A, Arrigo P, Di Lisi R, Ghiotto F, Scartezzini P.](#) (2002). The identification of a novel human homologue of the SH3 binding glutamic acid-rich (SH3BGR) gene establishes a new family of highly conserved small proteins related to Thioredoxin Superfamily. *Gene* 291, 233-239.
115. [Kostianovsky AM, Maier LM, Baecher-Allan C, Anderson AC, Anderson DE.](#) (2007). Up-regulation of gene related to anergy in lymphocytes is associated with Notch-mediated human T cell suppression. *J Immunol.* 2007 May 15;178(10):6158-63.
116. [Olsson LM, Lindqvist AK, Källberg H, Padyukov L, Burkhardt H, Alfredsson L, Klareskog L, Holmdahl R.](#) (2007). A case-control study of rheumatoid arthritis identifies an associated single nucleotide polymorphism in the NCF4 gene, supporting a role for the NADPH-oxidase complex in autoimmunity. *Arthritis Res Ther.* 9, R98.
117. [Ghebrehwet B, Peersckhe EI.](#) (2004). cC1q-R (calreticulin) and gC1q-R/p33: ubiquitously expressed multi-ligand binding cellular proteins involved in inflammation and infection. *Mol Immunol.* 41, 173-183.
118. [Yan Q, Malashkevich VN, Fedorov A, Fedorov E, Cao E, Lary JW, Cole JL, Nathenson SG, Almo SC.](#) (2007). Structure of CD84 provides insight into SLAM family function. *Proc Natl Acad Sci U S A.* 104, 10583-10588.
119. [Epting D, Vorwerk S, Hageman A, Meyer D.](#) Expression of rasgef1b in zebrafish. (2007). *Gene Expr Patterns* 7, 389-395.
120. [Maaser C, Egan LJ, Birkenbach MP, Eckmann L, Kagnoff MF.](#) (2004). Expression of Epstein-Barr virus-induced gene 3 and other interleukin-12-related molecules by human intestinal epithelium. *Immunology* 112, 437-445.
121. [Werth C, Stuhlmann D, Cat B, Steinbrenner H, Alili L, Sies H, Brenneisen P.](#) (2008). Stromal resistance of fibroblasts against oxidative damage: involvement of tumor cell-secreted platelet-derived growth factor (PDGF) and phosphoinositide 3-kinase (PI3K) activation. *Carcinogenesis* 29, 404-410.

Supplementary Table 2: *Pten*-responsive genes downregulated more than fourfold in the *Fsp-cre;Pten^{loxP/loxP}* vs. *Pten^{loxP/loxP}* primary mammary stromal cells

Gene Symbol	Gene name	Difference	Reference	Role
<i>Igfbp2</i>	insulin-like growth factor binding protein 2	69.3	122.	other
<i>Fmod</i>	fibromodulin	22.3	123.	ECM
<i>Prelp</i>	proline arginine-rich end leucine-rich repeat	19.1	124.	ECM
<i>Rerg</i>	RAS-like, estrogen-regulated, growth-inhibitor	9.7	125.	ECM
<i>Sned1</i>	sushi, nidogen and EGF-like domains 1	8.4	126.	ECM
<i>Atoh8</i>	atonal homolog 8 (Drosophila)	7.9	127.	other
<i>Efs</i>	Embryonal Fyn-associated substrate	6.7	128.	inflammation
<i>Fndc1</i>	fibronectin type III domain containing 1	6.2	129.	ECM
<i>Sfrp1</i>	secreted frizzled-related sequence protein 1	5.8	130.	ECM
<i>E430002G05Rik</i> (<i>Pamr1</i>)	peptidase domain containing associated with muscle regeneration 1		131.	ECM
<i>Wisp2</i>	WNT1 inducible signaling pathway protein 2	5.3	132.	other
<i>Ptprz1</i>	protein tyrosine phosphatase, receptor type Z, polypeptide 1	5.0	133.	ECM
<i>Gas6</i>	growth arrest specific 6	4.9	134.	inflammation
<i>Igf1</i>	insulin-like growth factor 1	4.7	135.	ECM
<i>Id4</i>	inhibitor of DNA binding 4	4.7	136.	other
<i>Smoc1</i>	SPARC related modular calcium binding 1	4.6	137.	ECM
<i>Pde8b</i>	phosphodiesterase 8B	4.6	138.	other
<i>Pcsk6</i>	proprotein convertase subtilisin/kexin type 6	4.4	139.	ECM
<i>Mfap4</i>	microfibrillar-associated protein 4	4.4	140.	ECM
<i>Syt13</i>	synaptotagmin XIII	4.3	141.	other
<i>Mgp</i>	matrix Gla protein	4.3	142.	ECM/calcification

Biological role affected by the genes downregulated in *Fsp-Cre;Pten^{loxP/loxP}*

122. [Heald AH, Kaushal K, Siddals KW, Rudenski AS, Anderson SG, Gibson JM. \(2006\).](#) Insulin-like growth factor binding protein-2 (IGFBP-2) is a marker for the metabolic syndrome. *Exp Clin Endocrinol Diabetes* 114, 371-376.
123. [Bi Y, Ehrichtiou D, Kilts TM, Inkson CA, Embree MC, Sonoyama W, Li L, Leet AI, Seo BM, Zhang L, Shi S, Young MF. \(2007\).](#) Identification of tendon stem/progenitor cells and the role of the extracellular matrix in their niche. *Nat Med.* 13, 1219-1227.
124. [Lewis M.](#) PRELP, collagen, and a theory of Hutchinson-Gilford progeria. (2003). *Ageing Res Rev.* 2, 95-105.
125. [Key MD, Andres DA, Der CJ, Repasky GA.](#) (2005). Characterization of RERG: An Estrogen-Regulated Tumor Suppressor Gene. *Methods Enzymol.* 407, 513-527.
126. [Leimeister C, Schumacher N, Diez H, Gessler M.](#) (2004). Cloning and expression analysis of the mouse stroma marker Snep encoding a novel nidogen domain protein. *Dev Dyn.* 230, 371-377.
127. [Ross MD, Martinka S, Mukherjee A, Sedor JR, Vinson C, Bruggeman LA.](#) (2006). Math6 expression during kidney development and altered expression in a mouse model of glomerulosclerosis. *Dev Dyn.* 235, 3102-3109.
128. [Donlin LT, Danzl NM, Wanjalla C, Alexandropoulos K.](#) (2005). Deficiency in expression of the signaling protein Sin/Efs leads to T-lymphocyte activation and mucosal inflammation. *Mol Cell Biol.* 11035-11046.
129. [Puente Navazo MD, Valmori D, Ruegg C.](#) (2001). The alternatively spliced domain TnFnIII A1A2 of the extracellular matrix protein tenascin-C suppresses activation-induced T lymphocyte proliferation and cytokine production. *J Immunol.* 167, 6431-6440.

130. [Barandon L, Couffignal T, Ezan J, Dufourcq P, Costet P, Alzieu P, Leroux L, Moreau C, Dare D, Dupl   C. \(2003\). Reduction of infarct size and prevention of cardiac rupture in transgenic mice overexpressing FrzA. Circulation, 108, 2282-2289.](#)
131. Cloning of cDNA encoding a regeneration-associated muscle protease whose expression is attenuated in cell lines derived from Duchenne muscular dystrophy patients. (2004). Nakayama Y, Nara N, Kawakita Y, Takeshima Y, Arakawa M, Katoh M, Morita S, Iwatsuki K, Tanaka K, Okamoto S, Kitamura T, Seki N, Matsuda R, Matsuo M, Saito K, Hara T. Am J Pathol. 164,1773-1782.
132. [Fritah A, Saucier C, De Wever O, Bracke M, Bi  che I, Lidereau R, Gespach C, Drouot S, Redeuilh G, Sabbah M. \(2008\). Role of WISP-2/CCN5 in the maintenance of a differentiated and noninvasive phenotype in human breast cancer cells. Mol Cell Biol. 28, 1114-1123.](#)
133. [Harroch S, Furtado GC, Brueck W, Rosenbluth J, Lafaille J, Chao M, Buxbaum JD, Schlessinger J. \(2002\). A critical role for the protein tyrosine phosphatase receptor type Z in functional recovery from demyelinating lesions. Nat Genet. 32, 411-414.](#)
134. [Son BK, Kozaki K, Iijima K, Eto M, Nakano T, Akishita M, Ouchi Y. \(2007\). Gas6/Axl-PI3K/Akt pathway plays a central role in the effect of statins on inorganic phosphate-induced calcification of vascular smooth muscle cells. Eur J Pharmacol. 556, 1-8.](#)
135. [O'Connor JC, McCusker RH, Strle K, Johnson RW, Dantzer R, Kelley KW. \(2008\). Regulation of IGF-I function by proinflammatory cytokines: At the interface of immunology and endocrinology. Cell Immunol. doi:10.1016/j.cellimm.2007.09.010](#)
136. [Sikder HA, Devlin MK, Dunlap S, Ryu B, Alani RM. \(2003\). Id proteins in cell growth and tumorigenesis. Cancer Cell 3, 525-530.](#)
137. [Gersdorff N, M  ller M, Schall A, Miosge N. \(2006\). Secreted modular calcium-binding protein-1 localization during mouse embryogenesis. Histochem Cell Biol. 126, 705-712.](#)
138. [P  rez-Torres S, Cort  s R, Tolnay M, Probst A, Palacios JM, Mengod G. \(2003\). Alterations on phosphodiesterase type 7 and 8 isozyme mRNA expression in Alzheimer's disease brains examined by in situ hybridization. Exp Neurol. 182, 322-334.](#)
139. [Nour N, Mayer G, Mort JS, Salvas A, Mbikay M, Morrison CJ, Overall CM, Seidah NG. \(2005\). The cysteine-rich domain of the secreted proprotein convertases PC5A and PACE4 functions as a cell surface anchor and interacts with tissue inhibitors of metalloproteinases. Mol Biol Cell. 11, 5215-5226.](#)
140. [Schlosser A, Thomsen T, Shipley JM, Hein PW, Brasch F, Torn  e I, Nielsen O, Skjodt K, Palaniyar N, Steinhilber W, McCormack FX, Holmskov U. \(2006\). Microfibril-associated protein 4 binds to surfactant protein A \(SP-A\) and colocalizes with SP-A in the extracellular matrix of the lung. Scand J Immunol. 64, 104-116.](#)
141. [Jahn JE, Ricketts SL, Coleman WB. \(2003\). Identification of candidate liver tumor suppressor genes from human 11p11.2 by transcription mapping of microcell hybrid cell lines. Int J Oncol. 22, 1303-1310.](#)
142. [Proudfoot D, Shanahan CM. \(2006\). Molecular mechanisms mediating vascular calcification: role of matrix Gla protein. Nephrology \(Carlton\) 11, 455-461.](#)

Supplementary Table 3: Primers list

qRT-PCR (Roche; Universal Probe Library Assay Design Center)

GENE	Link UPL	L / R	Left primer	Right primer	
CD48	NM_007649.4	L387/R441	cgagttgaagataaccctgga	tcgacgctcagcttattgatt	
C1orf38 (BC013712)	NM_001033308.2	L1698/ R1743	aagaaacagcagaacatacagagc	ctgcggttctacaacttgagg	
Ccl12	NM_011331.2	L100/R175	ccatcagtcctcaggtattgg	cttcggagcgtgaatcttct	
Ccl3	NM_011337.2	L119/R212	tgcccttgctgttcttctct	gtggaatcttcggctgtag	
Ccl4	NM_013652.2	L98/ R153	gccctctctcctcttggct	gaggggtcagagccattg	
Cdh1	NM_009864.2	L2282/R2325	atcctcgccctgctgatt	accaccgttctctccgta	
Csf1r	NM_001037859.1	L2355/R2410	ccgagggagactccagcta	gactggagaagccactgtcc	
Cybb	NM_007807.2	L1428/ R1481	tgccaacttctcagctaca	gtgcacagcaaatgattgg	
Ets-2	NM_011809.2	L210/ R264	cagtttctgtgggacactca	aaggggagcacagcaaca	
Fmod	NM_021355.2	L1038/ R1095	cagggcaacaggatcaatg	ctgcagcttggagaagtcat	
Gas6	NM_019521.2	L1608/R1661	ggatttgctactacaggctca	ttacttcccagggtgttcc	
Igfbp2	NM_008342.2	L664/R728	ggaggagcccaagaagtgtg	ggagatccgctccaggac	
Igfbp5	NM_010518.2	L1042/ R1098	ggcgagcaaaccaagataga	agggtcttctcagcatctcg	
IL1b	NM_008361.3	L632/ R679	tgtaatgaaagacggcacacc	tcttcttgggtattgctgg	
Itgb8	NM_177290.3	L2124/ R2170	acttctctgtccctatctcca	atctgccaccttcacactcc	
Krt23	NM_033373.1	L660/R700	tcatgaagaaacgcatgag	cctgaagtcactcggaag	
L4 (Rpl4)	NM_024212.2	L15/ R89	agcagccgggtagagagg	atgactctcccttttcggagt	
LacZ		L180/R226	ggcgattaagttgggtaacg	attcactggccgctgtttta	
Lcp1	NM_008879.2	L197 / R248	tcaacagacgggctgattc	agagcagcctgtcaagca	
Mmp12	NM_008605.3	L1247/R1299	ttgtggataaacactactggaggt	aatcagcttgggtaagca	
Mmp9	NM_013599.2	L1307 /R1374	acgacatagacggcatcca	gctgtggttctggtgtggtg	
Ncf2	NM_010877.4	L1037/ R1083	cttcggattcaccctcagtc	gaggtggtggaatatcgatt	
Pla2g7	NM_013737.5	L310/ R379	gtatccgggagtcagtgacag	agcgctgcagtttgagt	
Plek	NM_019549.1	L1114/ R1156	agtggatcaaagccatccag	tcagtgattctcgggtgcctc	
Prep	NM_054077.2	L82/ R133	cagaagagtgcccagagtc	atgccctcatgatccaggt	
VE-Cadherin	ENSMUST00000034339	L1589/R1645	gttcaagttgcccgaagaa	gtgatgtggcgggtgtgt	
Wisp2	NM_016873.1	L297/R362	tcctctgattctctcaatgg	gtgtccaaggacaggcaca	

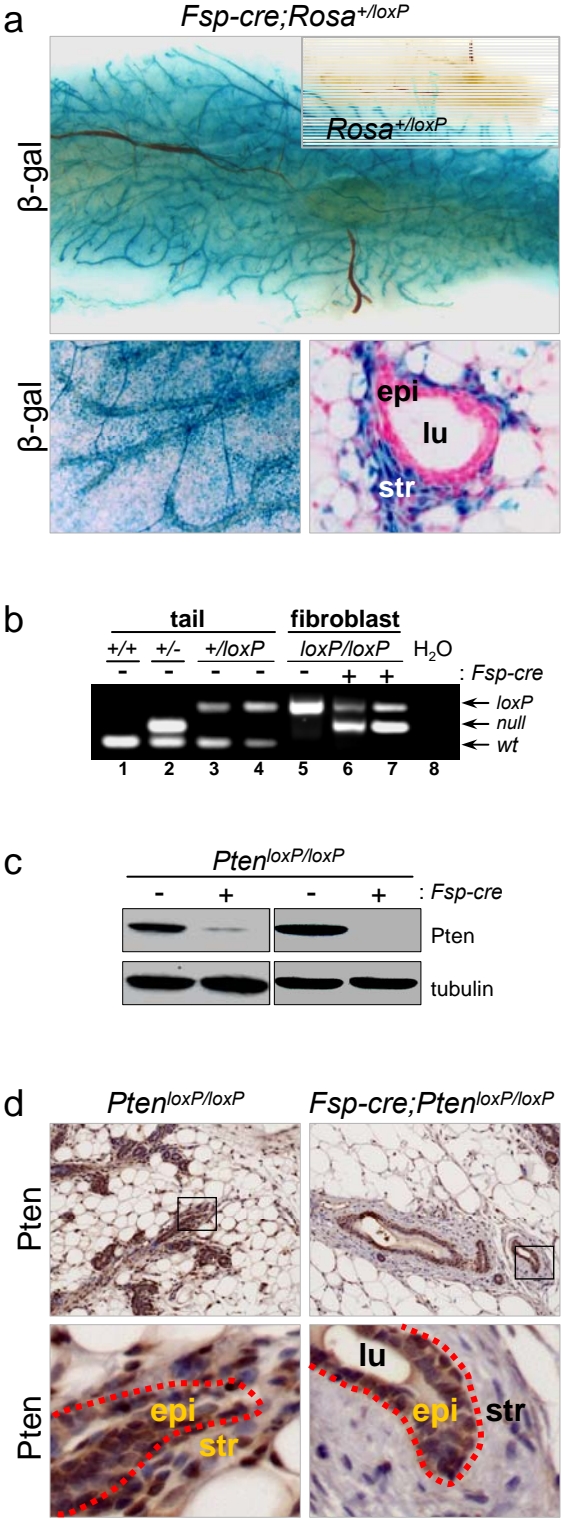
ChIP primers

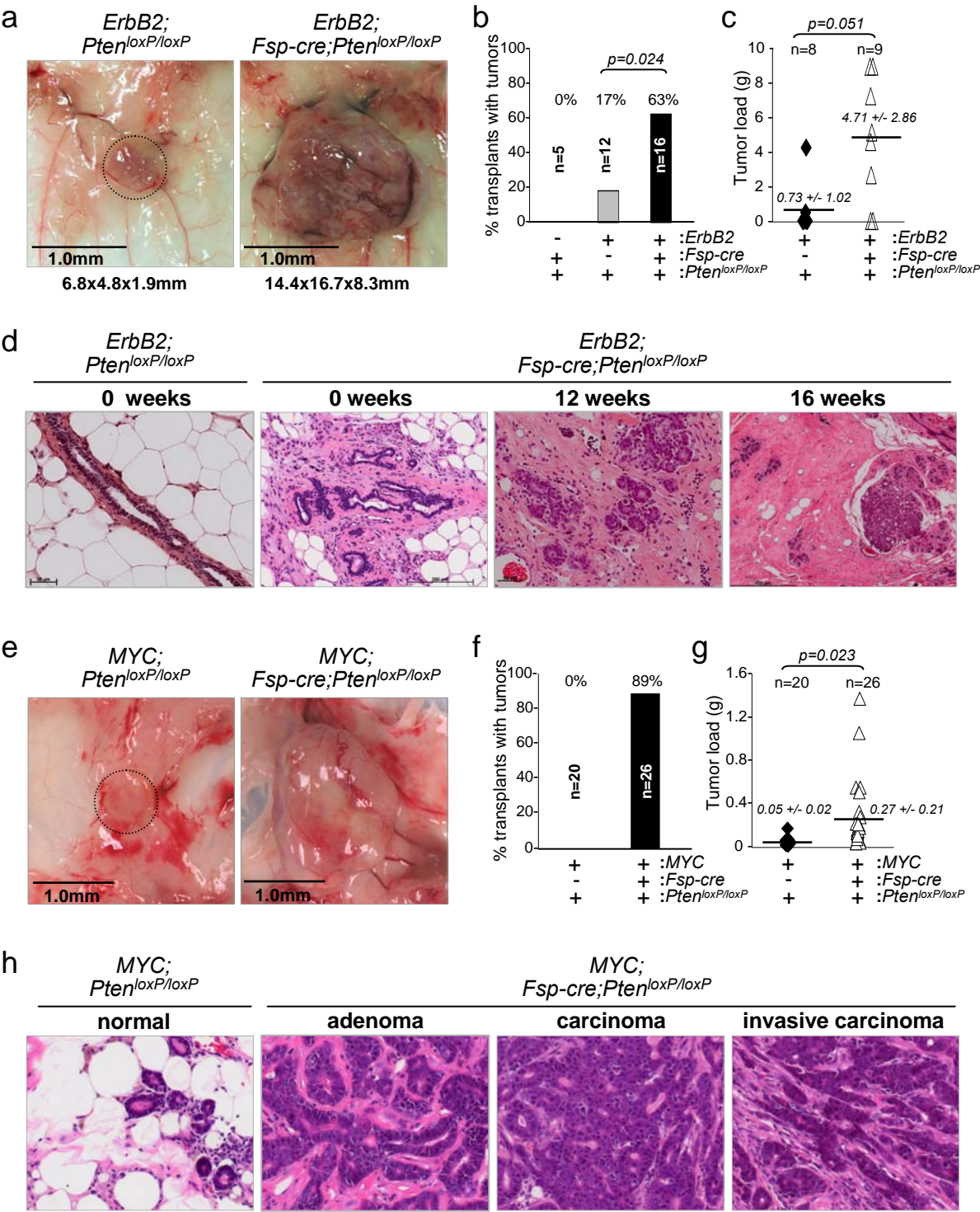
GENE	NCBI	L / R	Left primer	Right pri	
Mmp9	NT_039207	L381 / R325	gatggggcattcacctagc	gcctcagggtctccca	
Ccl3	NT_096135.5	L260 / R176	gtcctacctctctgctca	tcagctctcaactcgt	

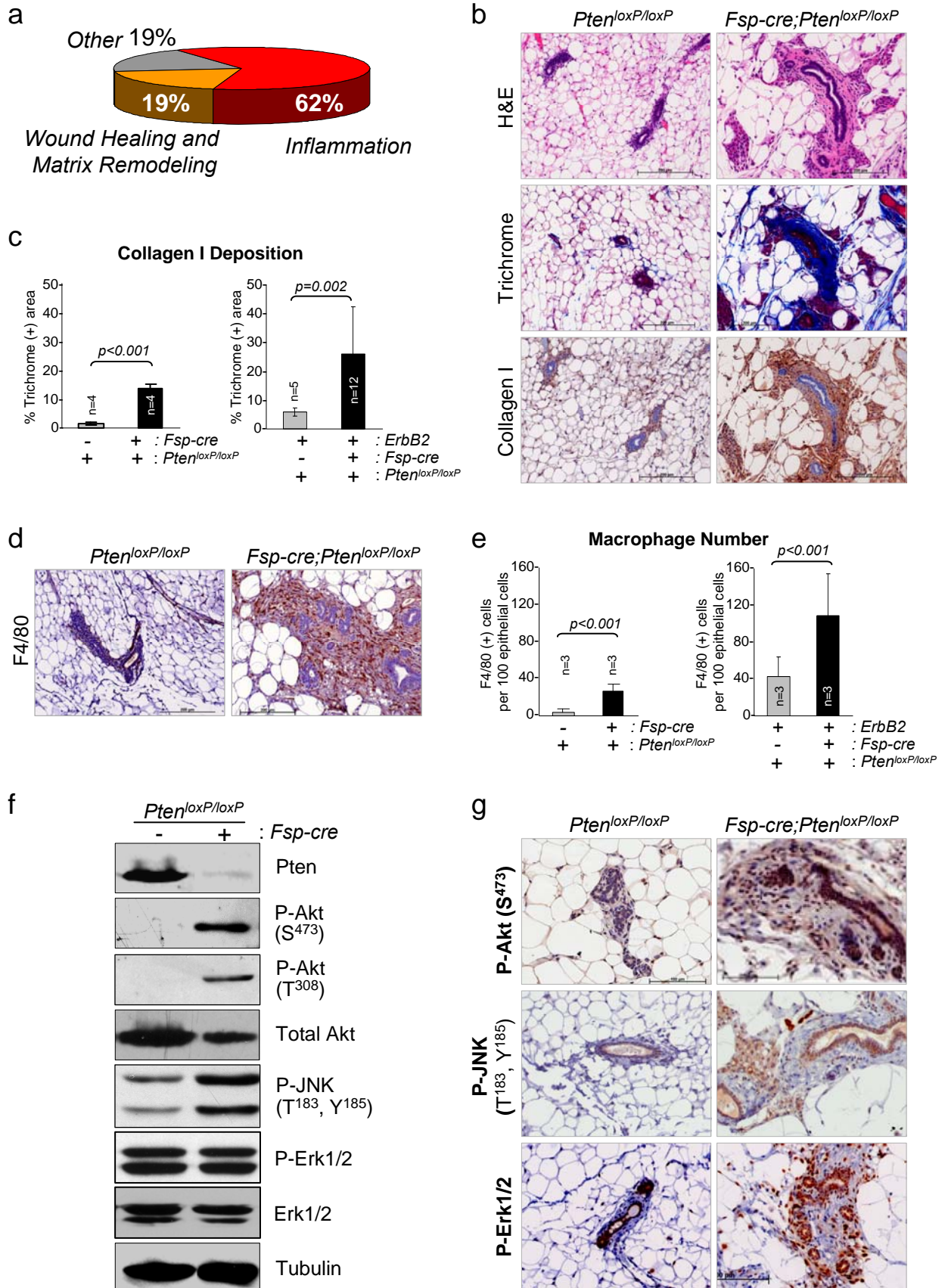
PCR genotyping

GENE	sens	Primers	Product size (bp)
MMTV-Neu	forward	GGAACCTTACTTCTGTGGTGTGAC	

MMTV-Neu	reverse	TAGCAGACACTCTATGCCTGTGTG	500bp
MMTV-PyMT	forward	CAGGGCGGGTCTGAGTCCATGG	
MMTV-PyMT	reverse	GGAAAGTCACTAGGAGCAGGG	200bp
Fsp-cre	forward	ATGCTTCTGTCCGTTTGCCG	
Fsp-cre	reverse	CAATGCGATGCAATTCCTC	1082bp
Ets2^{db}	forward	AATGACAAGACGCTGGGCGG	
Ets2^{db}	reverse	CGTCCCTACTGGATGACAGCGG	200bp
Pten^{loxP/WT}	common	GGGTTACACTAACTAAACGAGTCC	
Pten^{loxP}	loxP	GAATGCCATTACCTAGTAAAGCAAGG	300bp/220bp
Pten^{-/-}	deleted	GAATGATAATAGTACCTACTTCAG	280bp
Ets2^{loxP/WT}	common	CGCTTGCTAGGCAAGTGCTCTACC	
Ets2^{loxP}	loxP	GCTGACACAGGGTTTTGGTGTCTATGC	400/320bp
Ets2^{-/-}	deleted	CTAAGCCAGCCTGGCTACAGAACC	450bp
Rosa26^{loxP}	common	AAAGTCGCTCTGAGTTGTTAT	
Rosa26^{WT}	WT	GCGGGAGAAATGGATAT	550bp
Rosa26^{-/-}	transgene	GCGAAG-AGTTTGTCTCAACC	260bp
teto-myc	forward	GGAATGGCAGAAGGCAGG	
teto-myc	reverse	GCAGTAGCCTCATCATCACTAGATGG	580 bp
MMTV-rtTA	forward	AGTATGCCGCCATTATTACGAC	
MMTV-rtTA	reverse	CGATGGTAGACCCGTAATTGTT	170 bp







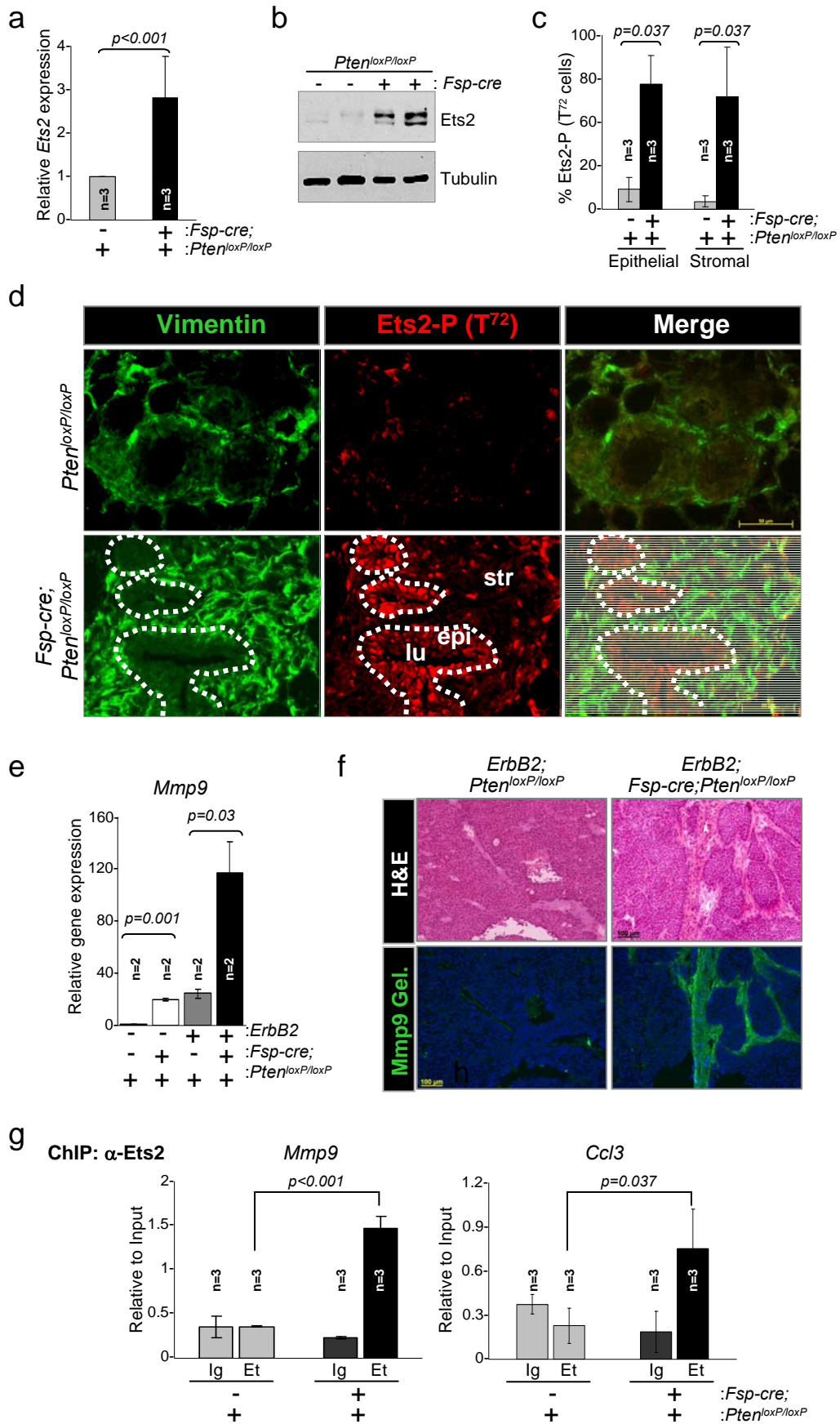


Figure 5

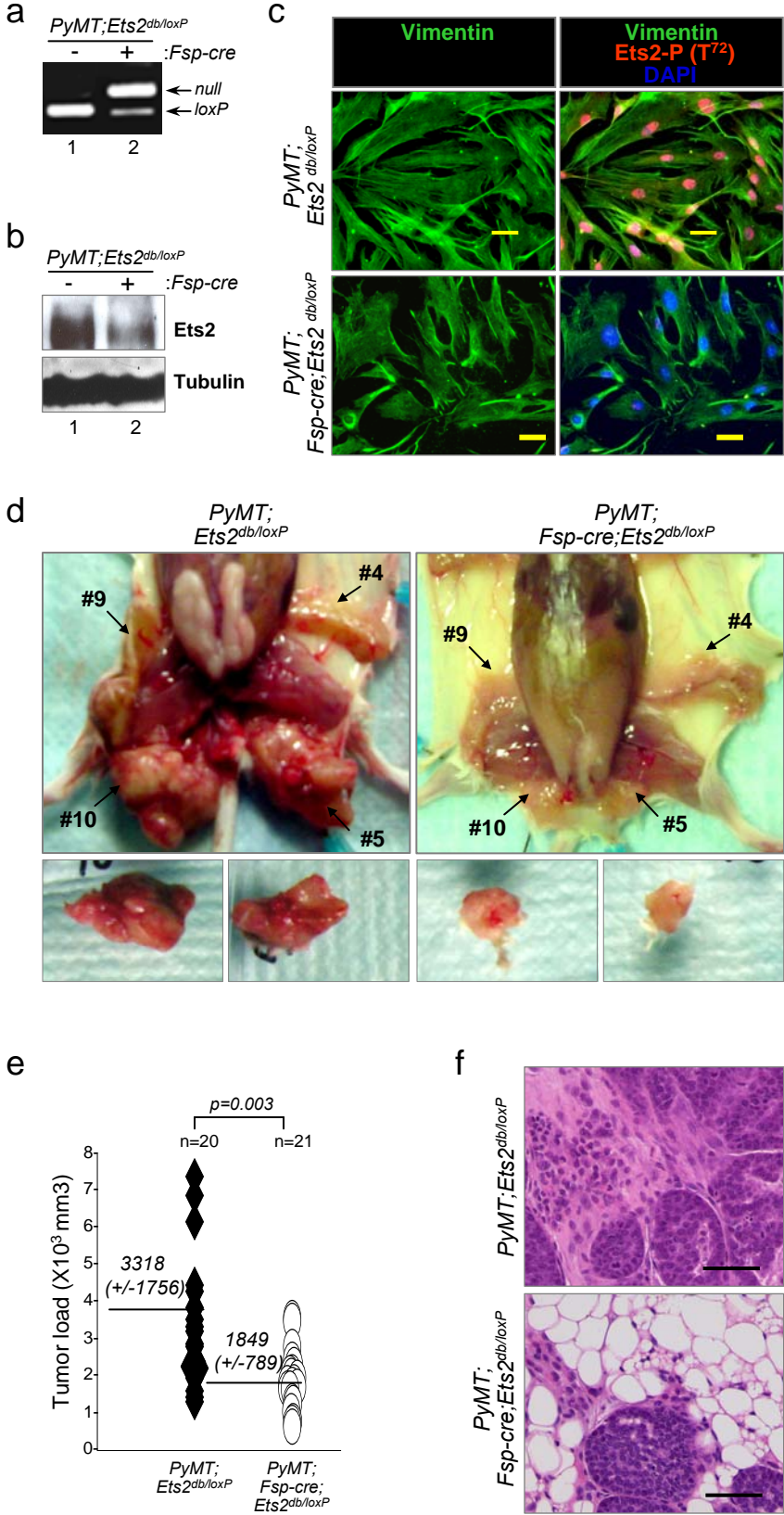
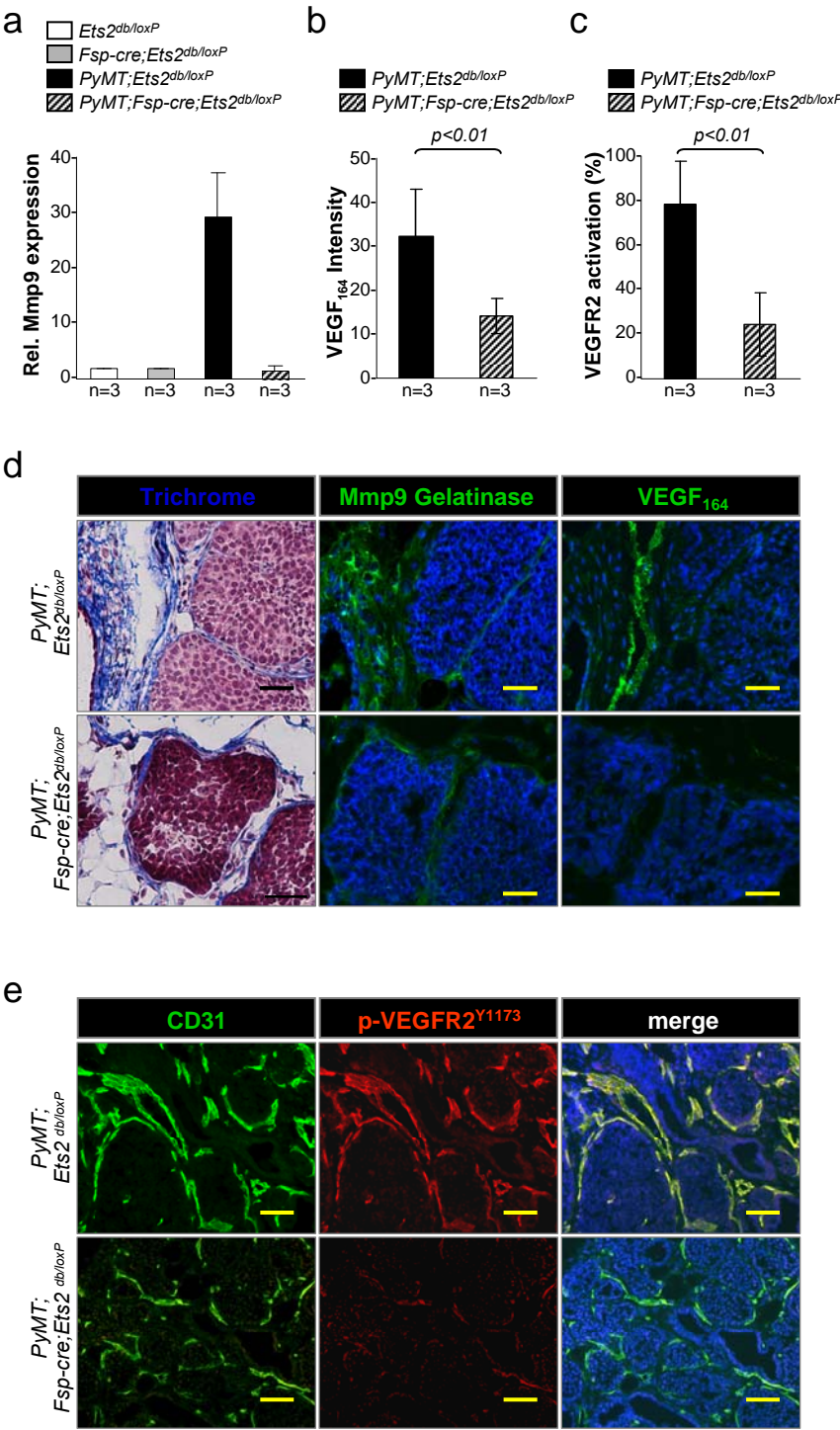


Figure 6



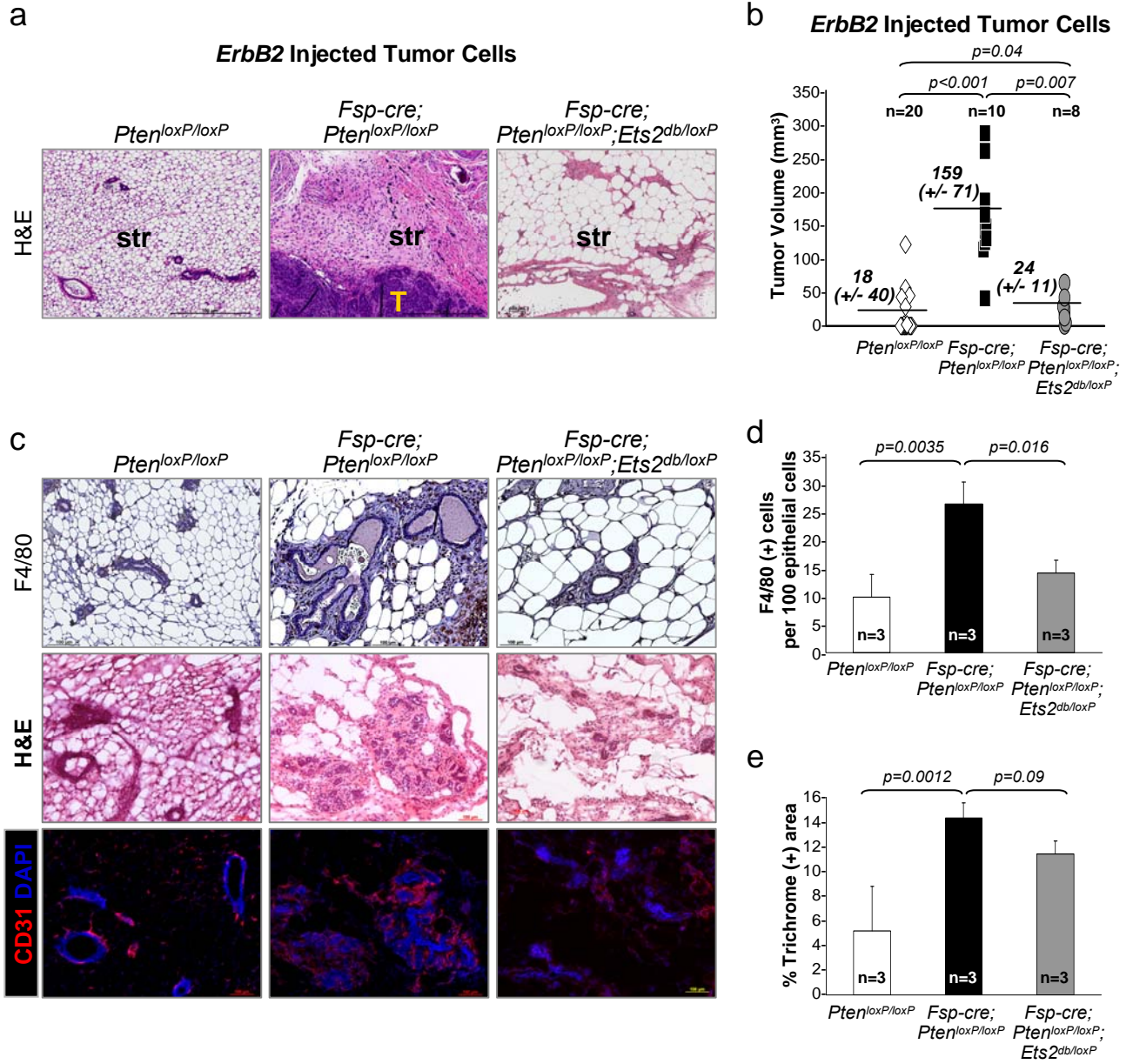
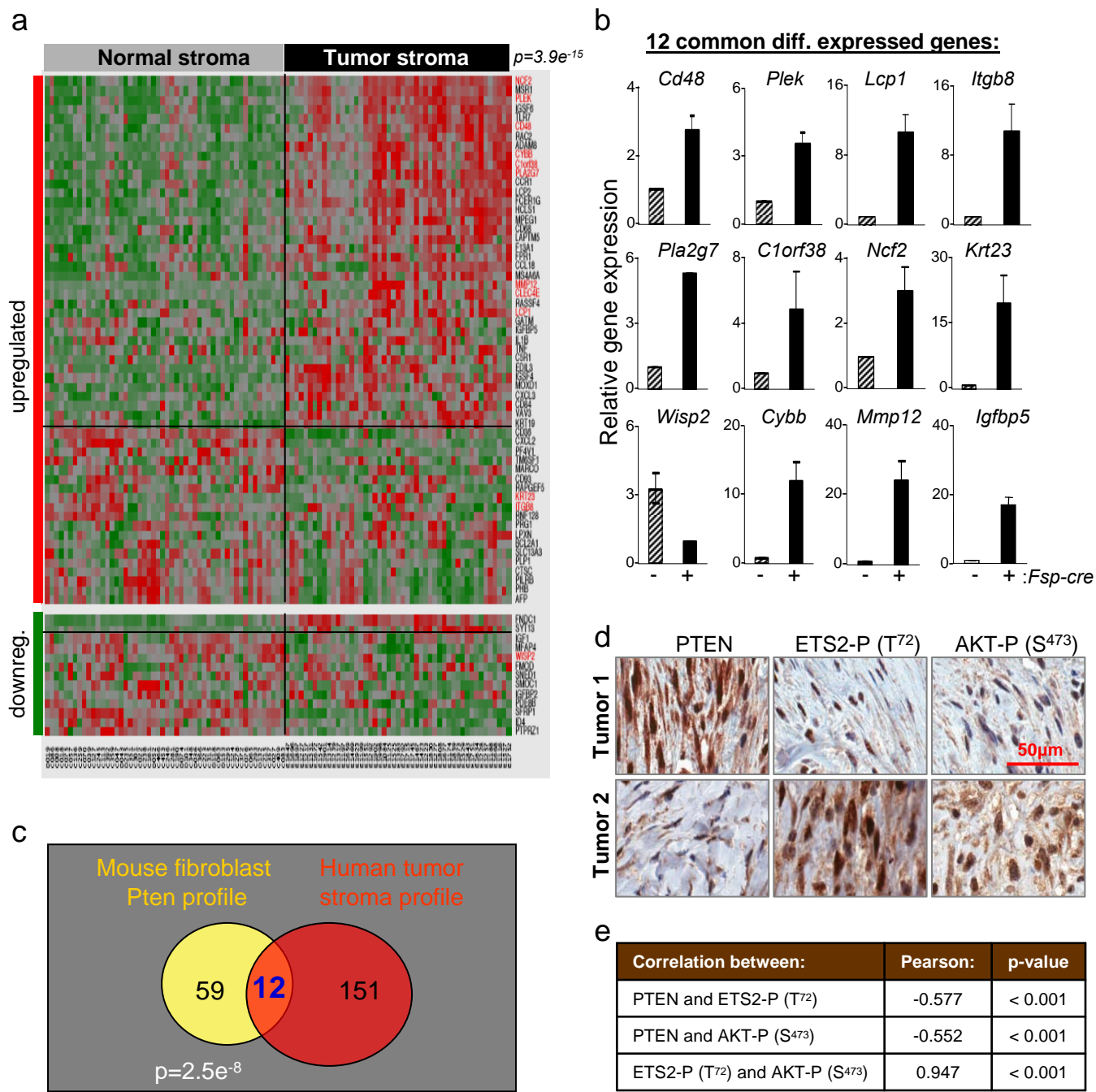


Figure 8



Generation of mice with Pten conditional knockout allele

